Received Date : 05-Feb-2016
Revised Date : 21-Aug-2016
Accepted Date : 03-Oct-2016
Article type : Themed Issue Paper

The Coniacian–Santonian sedimentary record in southern Tanzania (Ruvuma Basin, East Africa): Planktonic foraminiferal evolutionary, geochemical and palaeoceanographic patterns

MARIA ROSE PETRIZZO[†*], ÁLVARO JIMÉNEZ BERROCOSO[‡], FRANCESCA FALZONI[†], BRIAN T. HUBER[§], KENNETH G. MACLEOD[¥]

[†]*Dipartimento di Scienze della Terra "A. Desio", Università degli Studi di Milano, via Mangiagalli 34, 20133 Milano, Italy (*Corresponding author's e-mail: mrose.petrizzo@unimi.it).*

[‡]*Repsol Services Company, 2455 Technology Forest Blvd., Bldg. 5, The Woodlands, TX 77381, USA.*

[§] *Department of Paleobiology, MRC 121, Smithsonian Museum of Natural History, Washington, D.C. 20013, USA*

[¥]*Department of Geological Sciences, University of Missouri-Columbia, 101 Geological Sciences Bldg., Columbia, MO 65211, USA*

Associate Editor – Stuart Robinson

Running Title: Coniacian–Santonian sedimentary record in Tanzania

ABSTRACT

A 101 m thick stratigraphically complete late Coniacian–early Santonian (*ca* 89 to 83 Ma) sedimentary sequence drilled in Tanzania (Tanzania Drilling Project Site 39) allows, for the first time, examination of the planktonic foraminiferal biostratigraphy and evolution, the depositional history, and geochemical patterns of the subtropical–tropical Indian Ocean region. The sedimentary succession corresponds to an outer shelf to upper slope setting and is

This is an Accepted Article that has been peer-reviewed and approved for publication in the *Sedimentology*, but has yet to undergo copy-editing and proof correction. Please cite this article as an "Accepted Article"; doi: 10.1111/sed.12331

dominated by calcareous clayey siltstones and mudstones. The occurrences of Tethyan marker species enable application of the tropical biozonation including identification of the *Dicarinella concavata* and *D. asymetrica* Zones. In addition, Tanzania Drilling Project Site 39 is proposed as reference section for the Coniacian/Santonian boundary in the Indian Ocean with the boundary placed at the lowest occurrence of *Globotruncana linneiana* in agreement with the GSSP stratotype (Spain). The record at Tanzania Drilling Project 39 provides a unique opportunity to document the planktonic foraminiferal evolution in a subtropical marginal sea environment during a key period in their evolutionary history characterized by a major radiation among the deep-dwelling taxa. Combined documentation of lithological and geochemical changes (%$CaCO_3$, %C_{org}, $\delta^{13}C_{carb}$ and $\delta^{18}O_{carb}$) reveal a setting influenced by continental-derived nutrients in the *D. concavata* Zone (Lindi Formation) with a change to higher carbonate production and reduced surface water primary productivity in the overlying *D. asymetrica* Zone (Nangurukuru Formation). Planktonic foraminiferal assemblage changes mirror the depositional and geochemical trends and indicate a progressive shift from a more eutrophic to a more oligotrophic regime through time. At the local scale, this palaeoceanographic scenario is consistent with the deepening of coastal Tanzania in response to the Late Cretaceous marine transgression registered in south-east Tanzania. Because the tectonic evolution and sea-level rise along the East Africa continental margin is superimposed on the Coniacian–Campanian global long-term sea-level high, this study hypothesizes that the epicontinental invasion of blue waters may have favoured radiation among deep-dwelling taxa.

Keywords Biostratigraphy, Coniacian, evolution, geochemistry, palaeoceanography, planktonic foraminifera, Santonian.

INTRODUCTION

Palaeontological and geochemical evidence increasingly indicate that the Coniacian–Santonian interval represents the transition from the mid-Cretaceous extreme greenhouse characterized by elevated temperatures, increased volcanic activity, high sea level, and regional to global ocean anoxic events, to more temperate climatic conditions in the Campanian–Maastrichtian (e.g., Huber *et al.*, 1995, 2002; Clarke & Jenkyns, 1999; Wilson *et al.*, 2002; Frank *et al.*, 2005; Forster *et al.*, 2007; Hay, 2008, 2011; Bornemann *et al.*, 2008;

Robinson *et al.*, 2010; MacLeod *et al.*, 2011; Linnert *et al.*, 2014). Coincident with this climatic transition, planktonic foraminiferal assemblages underwent major compositional changes due largely to a pulse of diversification. The assemblage change is registered worldwide (e.g., Hart & Bailey, 1979; Wonders, 1980; Caron & Homewood, 1983; Hart, 1999; Premoli Silva & Sliter, 1999) and is marked by high rates of species diversification among existing genera (*Dicarinella*, *Marginotruncana* and *Contusotruncana*) and by the appearance of newly evolved keeled (*Globotruncanita* and *Globotruncana*) and biserial to multiserial (*Pseudotextularia*, *Ventilabrella* and *Sigalia*) genera. Extinctions are limited to one genus (*Whiteinella*), to a few species within the keeled *Marginotruncana* and *Dicarinella* genera, and to species within biserial genera. In addition, because the Coniacian–Santonian radiation phase is followed by the extinction of *Marginotruncana* and *Dicarinella* in the latest Santonian–earliest Campanian, the two evolutionary steps are traditionally regarded as due to a broader, major turnover (the so-called Santonian turnover) that affected all trophic groups within the planktonic foraminifera but was especially important in the history of more oligotrophic, keeled taxa (Wonders, 1980; Hart, 1980; Premoli Silva & Sliter, 1999).

Causes of the Santonian turnover, however, are still a matter of debate. Hypotheses proposed suggest that it could be related to: (i) tectonically forced changes in surface- and deep-water circulation (Premoli Silva & Sliter, 1999); (ii) the onset of the Late Cretaceous cooling trend during the late Santonian (Petrizzo, 2002) combined with taxa competition within particular depth habitats (Falzoni *et al.*, 2016); and (iii) the development of minor and regional anoxic events (i.e., Oceanic Anoxic Event 3; e.g. Schlanger & Jenkyns, 1976; Ryan & Cita, 1977; Arthur & Schlanger, 1979; Jenkyns, 1980; see Wagreich, 2012, for an overview) in the Atlantic and adjacent epicontinental sea, which resulted in the enlargement of the ecological niches in the more oxygenated Tethys, Pacific and Indian oceans (Wagreich, 2009). One of the challenges to understanding the causes of this foraminiferal turnover is that the Santonian sedimentary record is often incomplete. That is, records at deep-sea drilling sites frequently show discontinuous sections (Sliter, 1992; Ando *et al.*, 2013) preventing rigorous documentation of the interval, thus complicating efforts to integrate palaeontological and climatic trends into regional and global frameworks.

Drilling in southern coastal Tanzania by the Tanzania Drilling Project (TDP) during recent years, however, has recovered a stratigraphically complete subsurface section from the late Coniacian through the early Santonian (TDP Site 39) (Jiménez Berrocoso *et al.*, 2015) that constitutes one of the best records of calcareous plankton evolution in the Indian Ocean.

Strata at TDP Site 39 are mainly comprised of calcareous mudstones deposited in an outer shelf to upper slope setting (Jiménez Berrocoso *et al.*, 2010a, 2012, 2015). Planktonic foraminifera are diverse, show a strong Tethyan affinity, and generally exhibit excellent shell preservation. Foraminiferal shells, though, are infilled by calcite throughout the interval sampled precluding generation of unbiased C-isotopic and O-isotopic data suitable for inferring palaeoenvironmental conditions. Nonetheless, both the complete sedimentary record of TDP Site 39 and its planktonic foraminiferal content provide an excellent opportunity to document Coniacian–Santonian foraminiferal evolutionary patterns in a palaeo-subtropical site from the western Indian Ocean.

This study presents biostratigraphic and quantitative assemblage data for planktonic foraminifera across the Coniacian–Santonian boundary interval from TDP Site 39 with the aim of: (i) identifying the base of the Santonian Stage in Tanzania; (ii) providing a detailed biostratigraphic analysis of the section; and (iii) documenting the changes in the population structure and the timing and extent of speciation and extinction events. All of these data are important for identifying potential causes that forced the evolution of planktonic foraminifera. Further, the observed faunal changes are studied along with lithological and geochemical data (bulk sediment $\%CaCO_3$, $\%C_{org}$, $\delta^{13}C_{carb}$ and $\delta^{18}O_{carb}$) from TDP Site 39 in the pursuit of a robust depositional and geochemical framework. The final goal here is to test whether changes in the composition of the foraminiferal assemblage parallel the environmental perturbations in the water column as detected by lithological and geochemical variations, and if local environmental changes mirror or are independent of broader scale signals.

MATERIALS AND METHODS

Upper Cretaceous marine successions of south-east Tanzania were deposited in the Mandawa and Ruvuma basins (Salman & Abdula, 1995) and are exposed between Kilwa and Lindi (Fig. 1). Detailed description of the regional geology, stratigraphy and tectonic evolution of the Tanzanian basins can be found in Balduzzi *et al.* (1992), Ernst & Zander (1993), Veeken & Titov (1996), Mpanda (1997), Kapilima (2003), Kejato (2003), Pearson *et al.* (2004), Nicholas *et al.* (2006, 2007) and Key *et al.* (2008). The lithostratigraphic and biostratigraphic data gathered from the 2007 to 2009 TDP drilling seasons provided new information on the stratigraphy of the Tanzanian margin and allowed a more refined stratigraphic subdivision of

the Upper Cretaceous sediments. Upper Albian to pre-Santonian cored sediments, dominated by dark grey claystones and clayey siltstones, are included in the Lindi Formation (Jiménez Berrocoso *et al.*, 2015), whereas the overlying Santonian–Maastrichtian sediments, consisting of calcareous siltstones and claystones with minor intercalations of sandstones, are assigned to the Nangurukuru Formation (Nicholas *et al.*, 2006).

The transition from the Lindi Formation into the Nangurukuru Formation was recovered in TDP Site 39 (Fig. 1). This site was drilled in 2009 and was located 7.8 km north of Nangurukuru Junction and 15 km north-west of Kilwa (UTM 37L 532485, 9032440), close to a surface sample yielding a highly diverse assemblage of Coniacian–Santonian foraminifera (Fig. 2). The drilling operations and methods used to perform the lithostratigraphic, biostratigraphic and chemostratigraphic analyses are described in Jiménez Berrocoso *et al.* (2010a, 2012, 2015). In the present work, the chemostratigraphic results correspond to an average sampling spacing of 4 m (one sample every two cores) for the bulk sediment $\%CaCO_3$ and $\%C_{org}$ content, and of about 0.2 to 0.5 m (two to five samples per core) for the bulk carbonate $\delta^{13}C_{carb}$ and $\delta^{18}O_{carb}$ (Supporting Information – Table 1).

The foraminiferal samples (68) were taken at about 1.0 m intervals and were disaggregated and washed with tap water over a 63 µm sieve. Foraminifera are common in the samples, and the washed residues also contain varying amounts of quartz, mica and aggregate grains. Planktonic forms occur in greater abundance than benthic forms. The stratigraphic distribution of foraminiferal species is reported in the Supporting Information (Table 2). The list of taxa with authors and years discussed in the text is included in the Supporting Information (*Taxonomic notes*) together with remarks on taxa identifications when needed. Taxonomic concepts for planktonic foraminiferal genera and species identification applied in this study follow the original species descriptions, Robaszynski *et al.* (1979; 1984), Petrizzo & Premoli Silva (2000), Petrizzo (2000; 2002; 2003), Petrizzo & Huber (2006a,b), Huber & Leckie (2011), Petrizzo *et al.* (2011), Falzoni & Petrizzo (2011), Falzoni *et al.* (2014, 2016), Haynes *et al.* (2015) and the CHRONOS online Mesozoic Planktonic Foraminiferal Taxonomic Dictionary (http://portal.chronos.org). The planktonic foraminiferal biozonation applied in this study follows Robaszynski & Caron (1995) and Premoli Silva & Sliter (1995).

Planktonic foraminifera abundance counts were completed for 42 samples (about one sample per core) using a split of the >63 µm size fraction of approximately the same volume. Benthic foraminiferal abundance counts were performed on 25 samples (1 sample every two

cores) using the same split where planktonic foraminifera were counted. The percentage of planktonic specimens in the total foraminifera assemblages was calculated as Planktonic specimens/(Planktonic+Benthic specimens) *100. Samples were scanned for the presence of biostratigraphic marker species where counting was not performed (Supporting Information – Table 2). Results of the planktonic foraminiferal counts are plotted as percentages of groups of taxa according to similarities in morphology and wall texture features. Species richness and generic richness is the number of species and genera within the counted aliquot, respectively. Speciation and extinction rates are calculated as follows: rate of speciation equals the number of lowest occurrences (LO) divided by species richness within a given sample, and rate of extinction equals the number of highest occurrences (HO) divided by species richness within a given sample.

RESULTS

Lithostratigraphy

Tanzania Drilling Project (TDP) Site 39 reached 101 m below the surface, and 40 cores with moderate to high completeness were recovered (Jiménez Berrocoso *et al.*, 2015). The lower part of the borehole (cores 40 to 30) was identified as belonging to the upper sector of the Lindi Formation, whereas the upper part of the borehole (cores 29 to 1) was assigned to the Nangurukuru Formation (Jiménez Berrocoso *et al.*, 2015) (Fig. 3).

Cores 40 to 30 (top Lindi Formation) are 29 m thick and are composed of olive grey to olive black, well-lithified, silty claystones with massive textures (Fig. 3A). However, fine to medium laminations (millimetre to centimetre-thick alternations of darker, more clay-rich parts with lighter, more calcareous parts) are observed in cores 40 to 35 (Fig. 3B). These structures are similar to the common fine laminations found in the Lindi Formation elsewhere in south-eastern Tanzania (Jiménez Berrocoso *et al.*, 2010a, 2012, 2015).

The transition from the Lindi Formation into the overlying Nangurukuru Formation is marked by a gradational contact in cores 30 to 29 (Jiménez Berrocoso *et al.*, 2015) (Fig. 3). Above, cores 29 to 1 constitute 71 m of section and are here subdivided into two different lithological intervals (Fig. 3). The lower lithological interval (cores 29 to 14) is 45 m thick and exhibits olive grey to dark greenish grey, calcareous, clayey siltstones. It is characterized by alternating fabrics consisting of centimetre-thick, dark grey, clay-rich, commonly bioturbated siltstones intervening with light grey, rarely bioturbated siltstones in cores 28 to

24 and cores 21 to 14 (Figs 3C and 3D; see also fig. 13a–d in Jiménez Berrocoso *et al.*, 2015). The contacts between the two fabrics are usually gradational although sharp boundaries may occur. Burrows are present and are usually parallel to bedding; they have larger diameters (1 to 2 cm) in the darker intervals than in the lighter parts (<1 cm). The upper lithological interval (cores 13 to 1) is 26 m thick and includes olive grey, massive, calcareous, clayey siltstones, with common reddish oxide stains in cores 6 to 2. The oxide stains are due to modern weathering and increase in abundance through cores 13 to 7 (Fig. 3E). The down-core extent of Fe stains (core 13) is interpreted as the lower limit of modern weathering.

Finally, TDP Site 39 exhibits millimetre to centimetre-thick layers of carbonate-cemented siltstones (Fig. 3F); they occur occasionally throughout the entire borehole but are more frequent between cores 35 and 33. These layers may show sharp and irregular bases in addition to occasional ripple cross laminations. Their origin could be related to transport of silt-sized grains by sporadic bottom currents (see *Lithological inferences* section).

BIOSTRATIGRAPHY

Planktonic foraminifera are abundant in TDP Site 39 and, although infilled by calcite cements and/or pyrite, calcareous tests are remarkably well-preserved and shells often preserve their original wall texture. The lower part of the borehole (from bottom depth to 70.18 m) is included in the *Dicarinella concavata* Zone due to the absence of *D. asymetrica* and the presence of common to abundant marginotruncanids and dicarinellids. The interval from 70.18 to 0 m is assigned to the *Dicarinella asymetrica* Zone based on the consistent presence of the zonal species and common and large-sized marginotruncanids (for example, *M. undulata*, *M. angusticarenata*, *M. sinuosa*) (Supporting Information – Table 2; Fig. 4).

Assemblages suggest a high rate of diversification, with the appearance of six genera and several species that in stratigraphic order (Fig. 4) include *Pseudotextularia nuttalli* at 91.18 m (TDP 39/36-3, 1 to 25 cm), *Ventilabrella eggeri* at 79.18 m (TDP 39/32-1, 1 to 25 cm), *Dicarinella asymetrica* at 70.18 m (TDP 39/29-3, 1 to 25 cm), *Globotruncanita stuartiformis* and *Contusotruncana morozovae* at 69.18 m (TDP39/29-2, 1 to 25 cm), *Globotruncanita elevata* at 57.18 m (TDP 39/25-2, 1 to 25 cm), ‘*Heterohelix’ papula* at 36.69 m (TDP39/18-2, 48 to 80 cm), *Sigalia carpatica* at 29.18 m (TDP 39/16-1, 1 to 24 cm), *Costellagerina pilula* and *Sigalia decoratissima* at 28.73 m (TDP 39/15-1, 26 to 50 cm),

Globotruncana linneiana at 22.45 m (TDP 39/11-1, 25 to 54 cm), and *Globotruncana arca* at 18.76 m (TDP 39/9-1, 25 to 56 cm). There are also a number of highest occurrences. Within the genus *Dicarinella*, the following four species disappear: *D. canaliculata* at 68.20 m (TDP 39/29-1, 1 to 28 cm), *D. imbricata* at 59.18 m (TDP 39/26-1, 1 to 25 cm), *D. marginata* at 22.45 m (TDP 39/11-1, 25 to 54 cm) and *D. concavata* at 12.48 m (TDP 39/6-1, 25 to 60 cm). *Marginotruncana schneegansi* shows its highest occurrence at 61.18 m (TDP 39/26-3, 1 to 25 cm). The last representatives of the genus *Whiteinella* disappear at 21.64 m (TDP39/10-2, 47 to 70 cm). Finally, among the biserial planktonic foraminifera, two species disappear, *Planoheterohelix praenuttalli* at 65.18 m (TDP39/28-1, 1 to 25 cm) and *Huberella huberi* at 64.18 m (TDP39/27-3, 1 to 25 cm). Benthic foraminifera are a minor component of the assemblages. The lowest occurrence of *Neoflabellina gibbera* was recorded at 25.69 (TDP39/13-2, 30 to 57 cm). Additional rare specimens assigned to *Neoflabellina* sp. have been found in younger stratigraphic levels (Supporting Information – Table 2).

CHEMOSTRATIGRAPHY

Bulk %$CaCO_3$ and %C_{org}

The %$CaCO_3$ of TDP Site 39 ranges from 12 to 50% (average = 27% ± 12%, 1 s.d.; Jiménez Berrocoso *et al.*, 2015) and its vertical profile can be subdivided into at least two different parts (Fig. 5). The lower part extends from core 40 to 30 and exhibits an average value of *ca* 15% and relatively small variations (from 10 to 21%). An increase to values of *ca* 40% in $CaCO_3$ occurs in core 29, near the boundary between the Lindi Formation and the Nangurukuru Formation. The overlying interval has higher values and higher variability in %$CaCO_3$ than the interval below. The %$CaCO_3$ average 25 to 30% in the Nangurukuru Formation samples and range from 17 to 50%; highest values were found in cores 21 to 13. Despite its higher variability, the %$CaCO_3$ of the Nangurukuru Formation never returns to the low values consistently measured on samples from the underlying Lindi Formation. The %C_{org} ranges from 0.1% to 0.4% (average = 0.2% ± 0.1%, 1 s.d.; Jiménez Berrocoso *et al.*, 2015) and its concentration decreases from 0.4 to 0.2% at the level of the increase in $CaCO_3$ (core 29) near the contact of the Lindi Formation with the Nangurukuru Formation (Fig. 5).

Bulk $\delta^{13}C_{carb}$ and $\delta^{18}O_{carb}$

The bulk carbonate isotopes reveal changes that often correlate with the lithological, $\%CaCO_3$ and $\%C_{org}$ changes. The $\delta^{13}C_{carb}$ values range from -2.43 to 1.70‰ (average = 0.33‰ ± 0.72‰, 1 s.d.) and can be subdivided into at least five distinct intervals (Fig. 5). The first interval (1) runs from cores 40 to 28 (bottom hole to 66.5 m) and exhibits a negative $\delta^{13}C_{carb}$ trend that ends near the bottom of the Nangurukuru Formation, close to the level where there is an increase in $\%CaCO_3$ and a 0.2% decrease in $\%C_{org}$. The second interval (2) ranges from cores 28 to 24 (66.5 to 53.5 m) and exhibits a 3‰ positive change at the base, followed by a general negative trend (up to 53.5 m) that is punctuated by sharp negative excursions. This interval includes lithologies that show the aforementioned alternating fabrics with burrows. The third interval (3) shows a positive $\delta^{13}C_{carb}$ trend up section, which spans cores 23 to 22 (53.5 to 47.5 m) where lithologies have a dominantly massive texture. Above, the fourth interval (4) from 47.5 to 27 m (cores 21 to 14) has no apparent trend but exhibits a number of oscillations in $\delta^{13}C_{carb}$ values between 0.5‰ and 1.5‰ that may be associated with alternating lithological and bioturbation fabrics (similar to cores 28 to 24). That is, the alternating fabrics with burrows (cores 28 to 24 and cores 21 to 14) seem to show a $\delta^{13}C_{carb}$ profile with frequent and relatively sharp fluctuations. Finally, the fifth interval (5) from 27 m to the top of the hole (cores 13 to 1) exhibits relatively constant $\delta^{13}C_{carb}$ values punctuated by changes of up to 1.5‰, including a positive excursion (top of core 11), followed by a negative shift. An isolated negative $\delta^{13}C_{carb}$ spike observed in core 4 might be related to alteration due to modern weathering.

Compared to the $\delta^{13}C_{carb}$, the $\delta^{18}O_{carb}$ profile (Fig. 5) shows less variability (values range between -6.84‰ and -3.63‰; average = -4.65‰ ± 0.49‰, 1 s.d.). Two samples at 100.7 m and one sample at 47.0 m, however, show notably low $\delta^{18}O_{carb}$ values (-6.84‰, -6.62‰ and -6.54‰, respectively) that are explained either by calcite cements in the carbonate matrix or by localized calcite micro-fractures in the cored sediments (Jiménez Berrocoso *et al.*, 2010a, 2012). Similar to the $\delta^{13}C_{carb}$ record, though, the $\delta^{18}O_{carb}$ profile exhibits a slight negative trend from core 40 to near the boundary between the Lindi Formation and the Nangurukuru Formation (core 29). Above (cores 28 to 1), the $\delta^{18}O_{carb}$ is relatively constant and, only in the uppermost part (cores 4 to 1), presents a positive 1.5‰ change.

Base of the Santonian Stage in Tanzania

In order to test the completeness of the Coniacian–Santonian boundary interval in Tanzania the results from TDP Site 39 (Fig. 4) are compared to the Global Stratotype Section and Point (GSSP) for the base of the Santonian (Fig. 6; Cantera de Margas section, Olazagutia, northern Spain: Lamolda *et al.*, 2014, and references therein). The GSSP is marked by the lowest occurrence of the inoceramid *Cladoceramus undulatoplicatus* (= *Platyceramus undulatoplicatus*, see discussion in Gale *et al.*, 2007; Kennedy *et al.*, 2008) at 94.4 m in the Cantera de Margas section. Along with inoceramids (Gallemì *et al.*, 2007), the type section exhibits microfossil events (Melinte & Lamolda, 2007; Peryt & Lamolda, 2007; Lamolda *et al.*, 2007) and a negative 0.3‰ excursion in $\delta^{13}C_{carb}$ (Lamolda & Paul, 2007; Lamolda & Paul, 2009) that, together, have provided the basis for correlation with sites elsewhere (e.g. Jenkyns *et al.*, 1994; Jarvis *et al.*, 2006; Gale *et al.*, 2007; Takashima *et al.*, 2010; Voigt *et al.*, 2010; Wendler, 2013; Sprovieri *et al.*, 2013). Specifically, the Coniacian/Santonian boundary in the type section has been placed 4 m below a short-term positive $\delta^{13}C$ excursion correlated to the Michel Dean event and about 18 m above high $\delta^{13}C$ values correlated to the upper Coniacian Kingsdown event (Figs 6 and 7A).

Compared to the type section, no specimens of *C. undulatoplicatus* were identified in TDP Site 39 or in other localities in Tanzania, South Africa (Kennedy *et al.*, 2008; Kennedy & Klinger, 2014) and Madagascar (Walaszczyk *et al.*, 2014). Nevertheless, in the Madagascan sequence, which contains the most complete and rich ammonite and inoceramid record of the Upper Cretaceous successions described to date from the Southern Hemisphere, the appearance of the genus *Cladoceramus* is regarded as a good proxy for the base of the Santonian and is probably isochronous between Madagascar and the Euramerican biogeographic region (Walaszczyk *et al.*, 2014).

Comparison of the planktonic and benthic foraminiferal bioevents at TDP Site 39 with the published record from the Coniacian–Santonian boundary interval in the GSSP stratotype section highlights significant similarities, such as the same order of appearances of marker species *S. carpatica*, *C. pilula, N. gibbera* and *G. linneiana* within the *D. asymetrica* Zone (Figs 4 and 6). Major discrepancies in the foraminiferal record are not observed apart from the absence of single keeled globotruncanids (*G. stuartiformis* and *G. elevata*) in the Spanish record.

The $\delta^{13}C_{carb}$ profile at TDP Site 39 (Figs 5 and 7) shows a number of positive and negative fluctuations of 1 to 2‰ throughout the entire section, but identification of chemostratigraphic tie-points in the Coniacian–Santonian boundary interval as recorded in the GSSP type section (Lamolda & Paul, 2009), in other European sections (English Chalk: Jarvis *et al.*, 2006; German Chalk: Voigt *et al.*, 2010; Italian Scaglia: Sprovieri *et al.*, 2013), or in the US Western Interior (Gale *et al.*, 2007) is uncertain. If some shifts in the carbon isotope record here are genetically related to shifts documented in the English Chalk sections, the best candidates for the Michel Dean and the Kingsdown events would be the positive excursions at 22 m and 65 m in TDP Site 39, respectively. However, the present authors argue that global shifts among oxidized and reduced reservoirs were not dominant variables controlling the bulk $\delta^{13}C_{carb}$ record. Rather, it is suggested here that differences among samples in the nature of the carbonate sampled, the sources of DIC of the water in which biogenic carbonate precipitated, and/or remineralization of organic matter and diagenetic changes in the sediment column are more important variables. Thus, the present authors feel the $\delta^{13}C_{carb}$ record does not meaningful constrain chronostratigraphy at TDP Site 39, and age control is entirely based on the microfossil events (Fig. 7A and B).

The correlation between TDP Site 39 and the GSSP type section shows that the sequence of common microfossil marker species is probably reliable. The best-fit regression line from a cross-plot using the lowest occurrence of *Lithastrinus grillii*, *Sigalia carpatica*, *Costellagerina pilula*, *Neoflabellina gibbera* and *Globotruncana linneiana* in the two localities provides a correlation coefficient of 0.92 (Fig. 7B). Because the highest occurrence of *Lithastrinus septenarius* is significantly offset from the regression line, further studies are needed to clarify its stratigraphic distribution.

Given the absence of *C. undulatoplicatus* in TDP Site 39 and the uncertainty in the identification of chemostratigraphic tie-points correlative with coeval Coniacian–Santonian records elsewhere, and because of the similarity of most microfossil events between the two sites, it is suggested here that the appearance level of *G. linneiana* (22.45 m, core 11) is currently the most reliable means of identifying the base of Santonian Stage in Tanzania.

Planktonic foraminiferal assemblages

Diversity and evolutionary rates

The diversity and relative abundance data presented in Fig. 8 demonstrate significant changes among foraminiferal assemblages at TDP Site 39. In the *D. concavata* Zone the percentage of planktonic foraminifera varies from 76 to 91% at the top of zone (core 30, top Lindi Formation), while it is generally >90% in the *D. asymetrica* Zone. The one exception in the *D. asymetrica* Zone is an anomalous sample from 14.47 m (TDP 39/7-1, 28 to 56 cm) that is dominated by quartz and aggregate grains and in which planktonic foraminifera only represent 76.5% of the assemblage. The number of genera progressively increases throughout the stratigraphic interval from a minimum of four genera in the *D. concavata* Zone to a maximum of 11 in the *D. asymetrica* Zone. Species richness varies from 10 to 32 and shows high amplitude fluctuations in the upper part of the section. The lowest number of species (10 species) observed in the *D. concavata* Zone at 92.18 m (TDP 39/37-1, 1 to 25 cm) corresponds to a very small washed residue (Fig. 8).

Speciation and extinction rates reflect well the diversification of planktonic foraminifera at the genus and species levels passing from an interval (from the bottom of the borehole to core 26) characterized by the appearance of three new evolving genera (*Pseudotextularia*, *Ventilabrella* and *Globotruncanita*) and the disappearance of some dicarinellid, marginotruncanid and biserial species up to an interval (from core 25 to 16) with the progressive appearance of new species without extinctions of existing species, especially within the keeled taxa (Fig. 4). The relatively high rate of speciation in the upper part of the section (cores 15 to 9) coincides with the appearance of three genera (*Sigalia*, *Costellagerina* and *Globotruncana*) in a relatively short stratigraphic interval (Figs 4 and 8).

Relative abundances

Species and genera are grouped in clusters according to their morphological and wall texture features (Fig. 8). The most important species are illustrated in Figures 9 to 12. Double-keeled taxa with raised umbilical sutures (*Marginotruncana*, *Contusotruncana* and *Globotruncana*) are the main component of the >125 μm fraction and dominate in the *D. concavata* Zone, where they make up to 70% of the assemblages. This phase is followed by a progressive decrease in relative abundance of these taxa up section to a minimum of 30% in the lower part of the *D. asymetrica* Zone. There is a slight increase among these taxa to about 40 to

60% in the topmost part of the section. Double-keeled taxa with depressed umbilical sutures (*Dicarinella*) show a consistent occurrence but are less abundant (10 to 20%) compared with the other double-keeled taxa. Trochospiral taxa with a moderately muricate or pustulose wall texture (*Muricohedbergella* and *Archaeoglobigerina*) occur throughout the stratigraphic section and fluctuate in abundance, but they never exceed 20% of the total assemblages. Planispiral taxa (*Globigerinelloides*) show a consistent occurrence and increase in abundance throughout the section reaching 20% of the total assemblage in a few intervals. Biserial taxa with depressed intercameral sutures (‘*Heterohelix’*, *Huberella*, *Pseudotextularia* and *Planoheterohelix*) are the main component of the <125 μm fraction and show high amplitude fluctuations. This group dominates within the *D. concavata* Zone, where they reach up to 70% of the assemblages followed by a progressive decrease up-section to minimum values of 10% in the upper part of the *D. asymetrica* Zone.

Significant changes in assemblage composition occur across the Coniacian–Santonian transition (cores 15 to 9) with the progressive increase in abundance of: (i) the single-keeled *Globotruncanita* (reaching a maximum value of 10%); (ii) a newly evolved group of biserial and multiserial taxa characterized by raised intercameral sutures (*Sigalia*); and (iii) the multiserial genus *Ventilabrella* with depressed intercameral sutures. In the same stratigraphic interval, trochospiral taxa with costellae (*Costellagerina*) appear but they never exceed 3% of the total assemblage. Trochospiral taxa with coarse pustules (*Whiteinella*) are rare in the *D. concavata* Zone, and show an abrupt increase in abundance within the *D. asymetrica* Zone where they reach a maximum abundance of 20% before their extinction.

DISCUSSION

Lithological inferences

The Upper Cretaceous sediments from south-east Tanzania have been interpreted as having been deposited in an outer shelf to upper slope environment below the storm wave base and influenced by relatively low-energy conditions. This interpretation was based on the abundance of open ocean taxa (common planktonic microfossils and sporadic occurrences of ammonites and bivalves), as well as the predominance of lithologies dominated by clay-sized and silt-sized particles, and on the overall scarcity of sedimentary structures especially those indicating traction transport (Jiménez Berrocoso *et al.*, 2010a, 2012, 2015; Petrizzo *et al.*, 2011; Falzoni *et al.*, 2013; Wendler & Bown, 2013; Wendler *et al.*, 2013; Haynes *et al.*,

2015; Haynes *et al.*, 2016, accepted). Superimposed on these low-energy depositional conditions, cores 30 to 29 from TDP Site 39 record one of the main lithological shifts in the subsurface of this region: the transition from the Lindi Formation into the Nangurukuru Formation near the boundary of the *D. concavata* and *D. asymetrica* Zones (Fig. 3).

The upper part of the Lindi Formation is recorded in cores 40 to 30 (Fig. 3) and consists of well-lithified, silty claystones with undisturbed fine laminations as the most common sedimentary structure (Fig. 3B). The latter has been interpreted as indicating a setting that experienced low levels of burrowing activity and low oxygen conditions in bottom waters and/or within the sediments (Jiménez Berrocoso *et al.*, 2015; Haynes *et al.*, 2016, accepted). Also, cores 40 to 30 present a lack of fabrics indicative of gravity transport and/or traction of grains (for example, erosive basal contacts, fining-upward trends and cross-laminations) which suggests that dominant depositional processes were subsurface water flows that held fine particles in suspension until dilution of the flows allowed these particles to settle (Jiménez Berrocoso *et al.*, 2015; Haynes *et al.*, accepted). Wind-driven transport of fine particles is possibly an additional potential transport route, but its influence in Tanzania is difficult to evaluate with the current dataset. In rare cases, cores 35 to 33 exhibit millimetre to centimetre-thick beds of carbonate-cemented siltstones that present sharp, irregular bases as well as cross-laminations near the top. The sharp, irregular bases may be the result of relatively higher-energy flows that partly eroded the sea floor and eventually deposited carbonate and/or siliciclastic, silt-sized particles. The cross-laminations suggest traction of grains by the same flows. Together, possible depositional mechanisms for these beds could be storm-wave currents, gravity-driven flows and/or any other current affecting the sea floor (for example, longshore currents). Regardless, the rare occurrence of these beds indicates low-energy conditions prevailed during deposition of cores 40 to 30 (top Lindi Formation) in TDP Site 39.

Unlike cores 40 to 30, cores 29 to 1 are assigned to the Nangurukuru Formation and present comparatively calcareous clayey siltstones (Fig. 3). The lower part of this interval (cores 29 to 14) is characterized by the existence of centimetre-thick, alternating fabrics; dark grey, bioturbated siltstones alternate with light grey, rarely bioturbated siltstones, in particular in cores 28 to 24 and cores 21 to 14 (Fig. 3C and D). Burrows are visible in the two fabrics but their abundance is higher and their diameter is larger (up to 2 cm) in the darker than in the lighter parts (<1 cm). Gradational contacts are normally seen between the two fabrics, although they may be sharp in a few places. The origin of these fabrics must have

been related to the activity of burrowing fauna, which probably was more intense during deposition of the darker siltstones based on their frequent bioturbation. The ultimate control on the burrowing activity, though, could be a combination of factors, for instance: (i) changes in sedimentation rate; and/or (ii) nutrient and/or oxygen level fluctuations in bottom waters and/or within the sediments. Also, the fact that some sharp contacts exist between the two fabrics suggests that the transition from/into the deposition of the two fabrics could have been relatively fast in some cases. Alternatively, the sharp contacts may represent an expression of a partly incomplete sedimentary record; i.e. where the sharp contacts occur, a small hiatus and/or bottom-current related erosion may be present (see Jiménez Berrocoso *et al.*, 2013, for comparable features).

The upper part of TDP Site 39 (cores 13 to 1) mainly shows massive textures and, similar to cores 29 to 14, is relatively calcareous compared to the Lindi Formation. Based on the fine-grained lithologies of the Nangurukuru Formation from TDP Site 39, the present authors suggest that a main depositional mechanism for this unit could also be subsurface flows that held fine particles in suspension until dilution of the flows allowed them to settle (Jiménez Berrocoso *et al.*, 2010a, 2012, 2015). In addition to their calcareous character, the observed lithologies in the Nangurukuru Formation (cores 29 to 1) (i.e. siltstones) are generally slightly coarser than those in the Lindi Formation (cores 40 to 30) (i.e. claystones). No data are available to infer more detailed lithological variations in these sediments (fo example, grain size measurements); however, based on the observations here, the Nangurukuru Formation at TDP Site 39 was deposited in a setting that experienced: (i) higher carbonate production (see *$CaCO_3$ and C_{org} inferences* section); (ii) relatively higher oxygen levels in bottom water and/or within the sediments (higher bioturbation abundance); and (iii) slightly higher energy conditions (slightly coarser lithologies). Finally, similar to the Lindi Formation, the occasional existence of carbonate-cemented siltstone layers with sharp bases in the Nangurukuru Formation (cores 29 to 1) suggests that this setting was affected, albeit infrequently, by relatively higher-energy, bottom currents.

$CaCO_3$ and C_{org} inferences

Both the %$CaCO_3$ and %C_{org} profiles exhibit important variability in TDP Site 39. In particular, the sharp increase in $CaCO_3$ and decrease in C_{org} from cores 30 to 28 are significant for this work because they correspond with the lithological transition from the

Lindi Formation into the Nangurukuru Formation (Figs 3 and 5). The present authors argue that the $\%CaCO_3$ and $\%C_{org}$ profiles from this site, including the shift in cores 30 to 28, reflect depositional rather than diagenetic trends. Firstly, no evidence of major carbonate redistribution during diagenesis has been found (for example, large dissolution and/or cementation events), although centimetre to sub-millimetre scale cementation occurred (i.e. carbonate-cemented layers and cements inside microfossils tests throughout the site). Second, the absence of major lows in $\delta^{18}O_{carb}$ coincident with highs in $\%CaCO_3$ (Fig. 5), an expected relationship for diagenetic carbonate equilibrated with low $^{18}O/^{16}O$ ratios in pore waters at elevated temperatures with increasing burial depth (e.g. Allan & Matthews, 1982; Steinhauff *et al.*, 1999), argues against large diagenetic effects and suggests that the $\%CaCO_3$ profile preserves depositional trends. Thirdly, degradation of the sedimented organic matter in TDP Site 39 probably led to a partial loss of C_{org} at the sea floor and during burial. However, no major redox fronts have been detected in the study site, a situation that may suggest the overall existence of similar degrees of organic matter degradation in different parts of these sediments; thus, preservation of the $\%C_{org}$ depositional trends. The slight, but progressive, decrease in $\%C_{org}$ from 19 m to the top of the borehole (Fig. 5) is located just within the weathering zone of this site and probably reflects a partial loss of C_{org} due to alteration by the modern subtropical weathering.

The increase in $\%CaCO_3$ at the transition from the Lindi Formation into the Nangurukuru Formation could be explained by an increase in seawater carbonate production and/or a decrease in carbonate dilution by detrital inputs. Distinguishing between these two scenarios is challenging because no mineralogical data that would help decipher changes in detrital inputs are available in the two units. Either scenario or both scenarios together could provide an acceptable explanation for this increase in $\%CaCO_3$. An alternative explanation invokes a deepening of the carbonate compensation depth occurring near the onset of the *D. asymetrica* Zone in core 29. However, the relatively shallow palaeodepth inferred for TDP Site 39 (200 to 300 m, Jiménez Berrocoso *et al.*, 2015) means the carbonate compensation depth would have had to shoal dramatically for fluctuations in its position to affect lithologies at TDP Site 39.

In addition to lower $\%CaCO_3$ in the Lindi Formation, its $\%C_{org}$ is high compared to the Nangurukuru Formation. The latter situation may be interpreted as evidence of higher C_{org} burial flux during deposition of the Lindi Formation. If true, this scenario could reflect higher fluxes of organic matter to the sea floor and/or higher sedimentation rates during

deposition of the Lindi Formation, both cases that would promote relatively rapid burial and preservation of the sedimented organic matter. The inferred low bottom-water oxygenation, based on the often-preserved fine lamination of the Lindi Formation, would increase the potential to preserve the sedimented organic matter. Near the base of the *D. asymetrica* Zone, however, the observed decrease in $\%C_{org}$ suggests that the C_{org} burial flux decreased, for which the interpreted higher bottom-water oxygen levels for the Nangurukuru Formation (perhaps promoted by comparatively abundant bioturbation) would have played a significant role in degrading the sedimented organic matter.

Isotopic inferences

Similar to the other records from this site, the isotopic profiles exhibit a major change near the contact between the *D. concavata* and *D. asymetrica* Zones (Fig. 5). Both the $\delta^{13}C_{carb}$ and $\delta^{18}O_{carb}$ profiles present negative, long-term trends that culminate near the base of the *D. asymetrica* Zone. The shift is more evident in the $\delta^{13}C_{carb}$ record than in the $\delta^{18}O_{carb}$ record, but the $\delta^{13}C_{carb}$ profile exhibits higher variability. Diagenetic overprinting of the isotopic values must have occurred during burial and was probably related to: (i) cementation and/or recrystallization of carbonate grains leading to a decrease in their $^{18}O/^{16}O$ ratio; and (ii) incorporation of ^{12}C-rich remineralized organic carbon into carbonate cements. In addition, changes in oceanographic details could have affected carbon sources and cycling as well as the isotopic composition of seawater. Nevertheless, the primary isotopic trends may have survived diagenesis. On the one hand, lower $\delta^{18}O_{carb}$ values would be expected in the intervals with higher $\%CaCO_3$, since more frequent recrystallization and/or cementation events tend to occur in the carbonate-rich intervals (see, for example, the discussion in Jiménez Berrocoso *et al.*, 2013). As mentioned above, however, no major lows in $\delta^{18}O_{carb}$ coincide with higher $\%CaCO_3$ and vice versa. Indeed, the negative trend in the $\delta^{18}O_{carb}$ profile along the *D. concavata* Zone is accompanied by a stable vertical trend in $\%CaCO_3$, a situation that does not support diagenesis as a mechanism to mutually explain the two metrics. On the other hand, lower $\delta^{13}C_{carb}$ would occur in those intervals with higher $\%C_{org}$; that is, higher $\%C_{org}$ would promote greater likelihood of incorporating remineralized ^{12}C-rich carbon into the diagenetic carbonates. The negative trend in the $\delta^{13}C_{carb}$ profile through the *D. concavata* Zone differs from the stable vertical trend in $\%C_{org}$ (Fig. 5), also suggesting that diagenesis is not a probable explanation for the two metrics.

The present authors suggest that the bulk $\delta^{13}C_{carb}$ and $\delta^{18}O_{carb}$ trends are integrated signals that preserve environmental signals and mainly responded to the signature of carbonates precipitated in surface waters as well as a diagenetic overprint that shifted all values lower. The gradual decline in $\delta^{13}C_{carb}$ throughout the *D. concavata* Zone might reflect increasing influence of ^{12}C-enriched, terrestrial runoff waters on the surface and/or mid-waters of TDP Site 39 (Jiménez Berrocoso *et al.*, 2015; Haynes *et al.*, 2016, accepted). Such a scenario would imply increased input of continental-derived nutrients offshore that would have promoted primary productivity and, thus, a higher flux of C_{org} to the sea floor for the Lindi Formation. A trend to higher and more stable $\delta^{13}C_{carb}$ values persists through most of the *D. asymetrica* Zone. This trend suggests less influence of ^{12}C-enriched terrestrial runoff, reduced inputs of continental-derived nutrients to surface waters and, thus, lower primary productivity and lower flux of C_{org} to the sea floor (i.e. lower $\%C_{org}$) for the Nangurukuru Formation.

A similar scenario would explain the long-term $\delta^{18}O_{carb}$ trends. The $\delta^{18}O_{carb}$ decline through the *D. concavata* Zone suggests increasing influence of ^{16}O-enriched sources of terrestrial runoff culminating near the base of the *D. asymetrica* Zone. Throughout the *D. asymetrica* Zone, the $\delta^{18}O_{carb}$ exhibits a stable long-term trend that is accompanied by relatively high $\%CaCO_3$ suggesting a decrease in continental inputs to the depositional site that would have facilitated lower carbonate dilution (i.e. higher carbonate content) for the Nangurukuru Formation.

Evolution of *Dicarinella asymetrica* and *Globotruncanita* in Tanzania and implications for global correlation

The diverse and well-preserved planktonic foraminiferal assemblages found across the Coniacian–Santonian boundary interval provide an opportunity to document the timing of evolution of marker species in terms of radiation within lineages (e.g. Wonders, 1980; Olsson *et al.*, 1999; Pearson *et al.*, 2006; Petrizzo & Huber, 2006a, b; Ando & Huber, 2007; Gonzalez-Donoso *et al.*, 2007; Georgescu & Abramovich, 2008; Georgescu & Huber, 2009; Huber & Leckie, 2011; Falzoni & Petrizzo, 2011; Soldan *et al.*, 2011, 2014; Huber & Petrizzo, 2014; Haynes *et al.*, 2015; Petrizzo *et al.*, 2015). Because a robust biostratigraphic framework requires correct identification of the stratigraphic occurrences of marker species, this study provides two examples of identification of evolutionary lineages in which the

lowest occurrence of the index species, which is quite rare in its early range, is accompanied by the presence of transitional morphotypes. If a detailed analysis of the composition of the assemblage is not performed, those morphotypes could be easily misinterpreted and regarded either as falling in the morphological variability of the ancestor or descendent species, or described as new species. As a consequence, the lowest occurrences of marker species could be erroneously claimed to be diachronous.

The appearance of the biozonal marker *D. asymetrica* is preceded by the presence of transitional forms with features that fall between *D. concavata* and *D. asymetrica* (Fig. 13). Those transitional forms differ from *D. concavata* by having a slightly developed periumbilical ridge on the first two to three chambers of the final whorl and are thus distinguished from *D. asymetrica* because they do not possess a fully developed periumbilical ridge. However, those specimens could be easily identified as weakly developed *D. asymetrica*, therefore resulting in an incorrect placement of the lower boundary of the *D. asymetrica* Zone. Remarkable among TDP Site 39 samples is the presence of scattered specimens of *D. asymetrica* showing a single peripheral keel (at 57.18 m and 33.18 m), which are interpreted as extreme morphotypes that are still within the *D. asymetrica* species concept based on other morphological similarities.

The decrease in abundance of *D. concavata* followed by its extinction at 12.48 m within the *D. asymetrica* Zone (Fig. 13) correlates with observations from the Betic Cordillera in southeast Spain (Linares Rodriguez, 1977), the eastern Indian Ocean (Exmouth Plateau, Petrizzo 2000) and the Mangyshlak Peninsula (Kopaevich *et al.*, 2007), and is consistent with the planktonic foraminiferal distributions and biozonation by Postuma (1971). In contrast, *D. concavata* is reported to disappear at the same level as *D. asymetrica* in the US Western Interior (north Texas, Gale *et al.*, 2008) and in the Tethyan record (Tunisia, Robasynski *et al.* 2000; Italy, Premoli Silva & Sliter, 1995; Coccioni & Premoli Silva, 2015; Southern Tibet, Wendler *et al.*, 2009). This discrepancy could be related to: (i) differences in sampling resolution so that species that become rare at the end of their stratigraphic ranges are not detected in the assemblage; (ii) poor preservation of specimens that prevent the identification of species; and (iii) local ecological and palaeonvironmental factors that may force the local exclusion of *D. concavata*. Therefore, the highest occurrence of *D. concavata* cannot be used as marker event if not supported by additional data.

At TDP Site 39, the presence of transitional morphotypes has also been observed that show relative stability and long stratigraphic ranges. Among these, particularly important specimens are the ancestral morphotypes that give rise to the single-keeled *Globotruncanita* lineage (Fig. 14). Throughout the stratigraphic interval studied, the occurrence of specimens that resemble *M. undulata* by having raised and V-shaped umbilical sutures and crescentic spiral chambers, but differ from that species by developing a planoconvex morphology similar to *G. stuartiformis* were observed. Those forms still show two narrow keels on the first chambers of the last whorl, but only one keel is present on the ultimate and penultimate chambers. In addition, a second group of morphotypes possessing morphological features closer to *G. stuartiformis* than to *M. undulata* but differing from *G. stuartiformis* by having a less convex umbilical side than other specimens assigned to *G. stuartiformis* are recorded within the assemblages. Both morphotypes, here named *Marginotruncana* cf. *undulata*, could be easily included either in *M. undulata* or in *G. stuartiformis* and could even be regarded as a new species. However, since they co-occur in the same assemblage and show a consistent stratigraphic range, both morphotypes are interpreted here as being ancestral to *G. stuartiformis* (Fig. 14).

The evolution from *G. stuartiformis* to *G. elevata* through an increased convexity of the umbilical side is probably faster than the *M. undulata–G. stuartiformis* transition as rare intermediate morphotypes were observed in the studied assemblages. At TDP Site 39 the species *stuartiformis* is the first representative of the single keeled *Globotruncanita* lineage whose radiation represents an important novelty in the evolutionary history of Late Cretaceous planktonic foraminifera. *Globotruncanita* appears slightly above the appearance of *D. asymetrica* in agreement with observations from the Transitional Province (Exmouth Plateau, Petrizzo, 2000) while in the Tethyan Ocean (Tunisia, Robasynski *et al.*, 2000; Italy, Coccioni & Premoli Silva, 2015; Southern Tibet, Wendler *et al.*, 2009) the species *elevata* predates *stuartiformis*. Reasons for the apparent diachronism across latitudes of the single keeled taxa and of their absence in the Spanish (Lamolda *et al.*, 2007) and peri-Caspian Region (Kopaevich *et al.*, 2007; Walaszczyk *et al.*, 2013) records, and their rarity/absence in the US Western Interior records (Gale et *al.*, 2007, 2008) may point to: (i) the scattered recovery of the new evolving species because of low sampling resolution; (ii) misidentification of the ancestral species; and (iii) particular ecological preferences of the single keeled globotruncanids that develop and diversify in specific palaeoenvironmental conditions (i.e. cool/deep waters: Abramovich *et al*., 2003; Falzoni *et al*., 2013, 2016).

Planktonic foraminiferal assemblage changes

Comparison of relative abundance, richness and evolutionary rates among planktonic foraminifera from TDP Site 39 provides evidence of the assemblage changes and clues to variations in the water column structure over the Tanzanian margin during the late Coniacian–early Santonian. Although the extent to which the assemblage changes are driven by regional compared to global environmental perturbations cannot be determined rigorously, TDP Site 39 faunal data represent a continuous and detailed record of the planktonic foraminiferal evolutionary trend that may help in interpreting global scale signals. Palaeoceanographic inferences derived from planktonic foraminiferal data have been based on the current knowledge of species palaeoecology directly inferable from shell morphology in analogy with living taxa and latitudinal distributions (e.g. Hart, 1980, 1999; Leckie, 1987; Premoli Silva & Sliter, 1999), and on the information on species depth stratification acquired by measuring oxygen ($\delta^{18}O$) and carbon ($\delta^{13}C$) stable isotopes from pristine to very well-preserved foraminiferal shells (e.g. Wilson *et al.*, 2002; Abramovich *et al.*, 2003; Bornemann & Norris, 2007; Petrizzo *et al.*, 2008; Ando *et al.*, 2010; MacLeod *et al*., 2013; Wendler *et al.*, 2013; Falzoni *et al.*, 2013, 2014, 2016). At TDP Site 39, two phases in planktonic foraminiferal evolution (Faunal Change 1 and Faunal Change 2; Figs 8 and 15) are seen based on both quantitative data and planktonic foraminifera palaeoecological preferences known to date. These evolutionary phases separate three main ecological intervals (Intervals A, B and C; Figs 8 and 15) each one characterized by a distinctive taxonomic composition and probably different palaeoecological conditions. Below, the major planktonic foraminiferal changes are discussed and their palaeoceanographic significance is highlighted.

Interval A (cores 40 to 30; Figs 8 and 15): The *D. concavata* Zone is dominated by keeled taxa (*Marginotruncana* and *Contusotruncana*) and by biserials (‘*Heterohelix’*, *Huberella*, and *Planoheterohelix*) that, together with rare *Pseudotextularia*, represent more than the 70% of the total planktonic foraminiferal assemblages. Keeled and biserial taxa show opposite fluctuations in abundance.

Double-keeled taxa are abundant in low latitude assemblages and are traditionally interpreted as the most specialized taxa (thermocline dwellers) adapted to more oligotrophic regimes (e.g. Hart, 1980, 1999; Caron & Homewood, 1983; Leckie, 1987; Leary & Hart, 1989; Premoli Silva & Sliter, 1999). However, isotopic data from exceptionally well-preserved planktonic foraminifera from Santonian–Campanian sequences recovered at TDP Sites 28 and 32 (Falzoni *et al.*, 2013) and from well-preserved foraminifera from the Exmouth Plateau

(ODP Leg 122, Hole 762C; Falzoni *et al.*, 2103, 2016) indicate that the habitat preferences of several *Marginotruncana*, *Contusotruncana* and *Globotruncana* species do not simply follow these generalities. Results indicate that some *Marginotruncana* species were adapted to shallower/warmer waters and are better interpreted as mixed layer dwellers rather than thermocline dwellers. Previous scattered isotopic data (Norris & Wilson, 1998; Abramovich *et al.*, 2003; Bice *et al.*, 2003; Bornemann & Norris, 2007) are consistent with this interpretation. Biserial taxa are mainly small-sized, widely distributed and cosmopolitan, exhibiting low dominance at low latitudes, and dominating high latitude assemblages (Herb, 1974; Krasheninnikov & Basov, 1983; Huber, 1990). Biserial taxa are supposed to have high reproductive potential and inhabit shallow and nutrient-rich waters close to the eutrophic part of the resource spectrum (Nederbragt *et al.*, 1998; Leckie, 1987; Hart, 1999; Premoli Silva & Sliter, 1999; Petrizzo, 2000; Abramovich *et al.*, 2003; Wendler *et al.*, 2013; Haynes *et al.*, 2015, among many others).

Muricohedbergella, *Archaeoglobigerina* and biconvex *Dicarinella* are minor components in Interval A, because the three genera together never reach 30% of the assemblages. Isotopic signals suggest that biconvex *Dicarinella* species (*D. hagni* and *D. imbricata*) lived close to the thermocline (Falzoni *et al.*, 2016), whereas *Muricohedbergella* and *Archaeoglobigerina* show a high degree of adaptation to different trophic regimes spanning the mixed layer (Huber *et al.*, 1995; Norris *et al.*, 2002; Wilson *et al.*, 2002; Bornemann & Norris, 2007) to the permanent thermocline (Norris & Wilson, 1998; Petrizzo *et al.*, 2008) or a broad depth-distribution overlapping with the deeper and/or shallower taxa (Price *et al.*, 1998; Falzoni *et al.*, 2016).

Globigerinelloides are generally rare and reach 4% of the assemblage only in the upper part of the interval. Their ecological preferences are uncertain as biogeographic data coupled with quantitative and isotopic data suggest a high degree of adaptation to different trophic regimes in between the mixed layer and the thermocline and from low to high latitudes (Huber *et al.*, 1995; Hart, 1999; Premoli Silva & Sliter, 1999; MacLeod *et al.*, 2001; Petrizzo, 2002; Norris *et al.*, 2002; Abramovich *et al.*, 2003; Petrizzo *et al.*, 2008). Evolutionary rates reflect the appearance of the genus *Pseudotextularia*, a mesotrophic dwelling taxon living in the mixed layer (Petrizzo, 2002; Abramovich *et al.*, 2003; Falzoni *et al.*, 2016), of *Ventilabrella* interpreted as living close to the thermocline (Abramovich *et al.*, 2003), and of intermediate forms in between *D. concavata* and *D. asymetrica* (Fig. 13) that inhabited warm/shallow layers of the water column (Falzoni *et al.*, 2016).

In interval A the dominance of keeled and biserial taxa and the rarity of other taxa might correspond to variations in the depth of the mixed layer and of the thermocline and/or to a reduced temperature vertical gradient. In addition, the opposite fluctuation in relative abundance of keeled versus biserial taxa might reflect changes in the availability of nutrients resulting from variation in the continental runoff and/or intensity of the coastal upwelling. However, interpreting fluctuations in the availability of nutrients is challenging because no parallel geochemical variations are observed. Therefore, the palaeoceanographic interpretation herein is exclusively based on the palaeoecological preferences of planktonic foraminifera, which point to dominantly mesotrophic conditions with alternating phases of disruption and construction of the thermocline. The presence of taxa (*Muricohedbergella*, *Archaeoglobigerina*, *Dicarinella* and *Globigerinelloides*) known to be adapted to different trophic regimes within the mixed layer and upper thermocline further supports this interpretation because altogether they never reach the 30% of the assemblages.

Faunal Change 1: The base of the *D. asymetrica* Zone (cores 29 to 27; Figs 8 and 15) coincides with the transition from the Lindi Formation into the Nangurukuru Formation and with major geochemical changes. Planktonic foraminiferal extinctions almost mirror originations, but a species turnover occurs among the deep-dwelling keeled taxa with the appearance of the new genus *Globotruncanita* (e.g. Hart, 1999; Caron & Homewood, 1983; Leckie, 1987; Premoli Silva & Sliter, 1999) and the disappearance of two species of biconvex *Dicarinella* (*D. canaliculata* and *D. imbricata*). The lowest occurrence of *C. morozovae,* whose palaeoecological preferences are uncertain, is also recognized in this interval. The upward decrease in relative abundance of keeled taxa balanced by the increase in relative abundance of the umbilico-convex *Dicarinella* (*D. concavata* and *D. asymetrica*), which inhabited shallow layers of the water column in the late Coniacian (Falzoni *et al.*, 2016), and by the increase of *Globigerinelloides* and trochospiral muricate taxa, suggests a transition to a thicker mixed layer.

Altogether, the observed faunal change results in increased diversity of the assemblage that probably reflects an increased stratification of the upper water column. Such conditions could be related to: (i) an increase of the vertical temperature gradient; (ii) reduced water mixing; and (iii) a reduced input from continental runoff and nutrient supply. At TDP Site 39, the latter interpretation is supported by the sharp increase in $\%CaCO_3$ (Figs 5 and 15) that may reflect diminished water turbidity and deepening of the photic zone that allow

increased vertical stratification, and thus increased availability of ecological niches to be occupied by planktonic foraminifera.

Interval B (cores 26 to 16; Figs 8 and 15): In this interval, the shallow water biserial taxa constituted more than 50% of the assemblages, whilst keeled taxa never reach 35% of the assemblages. A progressive increase in abundance of the deep dweller *Globotruncanita* and of the mixed layer umbilico-convex *Dicarinella* is recorded throughout the interval. Trochospiral muricate taxa progressively decrease and *Globigerinelloides* show low amplitude fluctuations. Interestingly, the more opportunistic planispiral and trochospiral muricate taxa reach minimum values between cores 19 to 17. In the same stratigraphic interval, the increase in relative abundance of the umbilico-convex *Dicarinella* and the abrupt increase in relative abundance of *Whiteinella* are observed, both interpreted as warm/shallow water taxa based on stable isotope data (Huber *et al.*, 1995, 1999; Bornemann & Norris, 2007; Falzoni *et al*., 2016), despite the fact that *Whiteinella* has been also associated with upwelling regions (Hart, 1999; Premoli Silva & Sliter, 1999). Evolutionary rates reflect the appearance of *G. elevata* and of the large biserial '*H.' papula*. While the former species is a thermocline dweller, the ecological preferences of the latter species are uncertain owing to lack of consistent data.

Assemblage changes in interval B reflect a progressive diversification and increase in relative abundance of taxa adapted to the mixed layer and to the upper thermocline indicating the development of a more stratified water column. The significance of the abrupt increase in abundance of *Whiteinella* is puzzling because it might either reflect eutrophy or an increase of the surface water temperature. Intriguingly, the peak in abundance of whiteinellids coincides with the interval of maximum $\%CaCO_3$ that might suggest a more oligotrophic regime. Therefore, based on the palaeoecological preferences of planktonic foraminifera and on the composition of the assemblages a dominantly mesotrophic to oligotrophic regime is inferred for this interval. This interpretation is consistent with the increase in abundance of the surface dweller taxa that could be related to an increase in sea surface temperature.

Faunal Change 2: Cores 15 to 9 record (Figs 8 and 15) a major evolutionary phase in planktonic foraminifera as originations exceed extinctions. The rapid and high rate of diversification occurs among deeper dwelling taxa with the appearance of *Sigalia* and

diversification of *Ventilabrella* both interpreted as living close to the thermocline (Abramovich *et al.*, 2003; Falzoni *et al.*, 2013) whilst the new evolving genus *Costellagerina* has been interpreted as an upper/summer mixed layer dweller (Petrizzo *et al.*, 2008; Ando *et al.*, 2010; Falzoni *et al.*, 2014). In addition, the isotopic signature of the new evolving species *G. linneiana*, measured on specimens from TDP Sites 28 and 32, suggest it was a seasonal thermocline or a winter mixed layer dweller (Falzoni *et al.*, 2013).

In terms of assemblage composition, the fluctuations in relative abundance of all taxa, together with the high evolutionary rate, might indicate that a broader water mass perturbation occurred. Specifically, a first phase characterized by an abrupt decrease in abundance of biserial taxa coupled with the abrupt increase in abundance of the shallowest surface water dweller *Whiteinella* are observed (Huber *et al.*, 1995, 1999; Bornemann & Norris, 2007) that may indicate direct competition among species within the upper mixed layer. In the same interval the highest rate of evolution of the deeper dweller taxa is seen. This phase is followed by a reverse situation marked by an abrupt increase in the abundance of the shallow water biserial taxa balanced by the decrease in relative abundance of the deeper dwellers and by the extinctions of the warm/shallow water *Dicarinella* species (*D. concavata* and *D. marginata*) and whiteinellids. Interestingly, the increase in abundance of biserial taxa and the extinction of whiteinellids coincide with a sharp drop in $\%CaCO_3$ that reaches values similar (17%) to those observed in Interval 1 (*D. concavata* Zone). Altogether, Faunal Change 2 is interpreted to include a first phase characterized by a well-defined sea surface stratification that is followed by a short term intensification of eutrophy (i.e. increased continental runoff and coastal upwelling) that abruptly disrupted the stable mixed layer and thermocline and might be associated with decreasing sea-surface temperatures.

Interval C (cores 8 to 11; Figs 8 and 15): The topmost interval is characterized by a progressive increase in diversity. The deeper dwelling species within the genera *Globotruncanita*, *Sigalia* and *Ventilabrella* show an increase in abundance. The lower mixed layer to thermocline dwellers (*Marginotruncana* and *Contusotruncana*) dominate the assemblages, whilst the most tolerant and opportunistic biserial taxa rarely reach 22% of the assemblages. Speciation and extinction rates are about evenly balanced.

The composition of the assemblages and the increase in genera and species richness reflect the development of new ecological niches suitable for the new taxa that could have evolved during the phase of increased stratification and/or replacement of niches occupied by species that became extinct. Both interpretations might reflect oligotrophic conditions and more thermally stratified surface waters.

Palaeoceanographic inferences and depositional conditions

Planktonic foraminiferal assemblage changes and radiation of the deep-dwelling taxa registered across the Coniacian–Santonian boundary interval in south-eastern Tanzania are well-documented at low latitudes and are correlative worldwide in coastal, open-ocean, organic carbon-poor, pelagic chalk settings (e.g. Hart & Bailey, 1979; Caron & Homewood, 1983; Hart, 1999; Premoli Silva & Sliter, 1999; Robaszynski *et al.*, 2000). The subtropical features of the assemblages at TDP Site 39 are in agreement with the palaeogeographic reconstructions that locate the Tanzanian margin at a palaeolatitude of about 30°S during the Late Cretaceous (Hay *et al.*, 1999). Circulation models for the Late Cretaceous (Bush & Philander, 1997; Poulsen *et al.*, 1998; Otto-Bliesner *et al.*, 2002; Hay, 2009) and Nd isotope data (Pucéat *et al.*, 2005) suggest the presence of a permanent westward flowing current (Equatorial Circumglobal Current) that ensured a low-latitude connection from the Pacific to the Tethyan Ocean and a southward surface flow active along East Africa reaching the Tanzanian margin. Such a current would explain why the Tanzanian assemblage shows a strong Tethyan affinity and records the radiation of the low latitude and deeper *Sigalia* species (Salaj, 1984; Nederbragt, 1990), which are absent in the Transitional Province (for example, Exmouth Plateau; Belford, 1983; Wonders, 1992; Petrizzo, 2000, 2002) and at high latitudes (for example, South Atlantic: Sliter, 1977; Huber, 1992; southern Indian Ocean: Petrizzo, 2001, 2003). However, the earlier appearance of the single keeled globotruncanids in Tanzania compared to the Tethyan record reveals the different timing of radiation of these deeper dwelling taxa across latitudes, and demonstrates that they first evolved in a subtropical epicontinental marginal setting when a major change in the depositional regime occurred, that is, the transition from the Lindi Formation (*D. concavata* Zone) into the Nangurukuru Formation (*D. asymetrica* Zone). Specifically, variations in bulk rock geochemistry and lithology at TDP Site 39 suggest a palaeoceanographic scenario influenced by relatively low-energy depositional conditions that evolved from relatively high inputs of

continentally derived nutrients throughout the *D. concavata* Zone, to higher carbonate production and reduced nutrient availability throughout the *D. asymetrica* Zone (Fig. 15).

In terms of water mass organization, planktonic foraminiferal data indicate a progressive shift from mesotrophic conditions with alternating phases of disruption and construction of the thermocline to a more stratified and oligotrophic water column associated with a definite mixed layer and a permanent thermocline (Fig. 15). The development of a stable thermocline implies a temperature gradient between surface and deeper waters that could be partly explained by increased water depth through time in Tanzania, for example, from an outer shelf to an upper slope setting. Deepening of the depositional site could have been accompanied by an invasion of oligotrophic waters, a situation that may be interpreted as the response to a widespread marine transgression on the Tanzania–Mozambique margin after the separation of India from Madagascar and the opening of the Mascarene Basin about 93 Ma (Salman & Abdula, 1995; Nicholas *et al.*, 2007; Key *et al.*, 2008). Increased vertical stratification of surface waters over these margins resulted in increased availability of ecological niches in the water column that were occupied by planktonic foraminifera.

The current knowledge that planktonic foraminiferal diversity parallels the global sea-level fluctuations of the Mesozoic (Hart & Bailey, 1979; Hart, 1999; Leckie, 2009) supports this explanation. During the mid-Cretaceous, calcareous oceanic plankton progressively invaded the epicontinental seas, probably in response to the long-term sea-level rise from the late Albian through to the Campanian (Hay, 2008). Moreover, the beginning of the sedimentation of the Cretaceous chalk in the Albian has been related to the combined effect of long-term sea-level rise and tectonic activity that may have increased the connection among oceanic basins and created a stable surface and deep water current system (Giorgioni *et al.*, 2015) suitable for the proliferation of calcareous plankton. After peak sea-level rise in the earliest Turonian (about 250 m above the present day mean sea level), sea level fell in the late Turonian by about 60 m, then a period of sea-level stasis, with long-term values varying only by about 20 m, characterized the Coniacian–Campanian time interval (Haq, 2014, and references therein). Expanded epicontinental seas, including in East Africa, during this long phase of eustatic high may have provided increased opportunities for planktonic foraminifera to diversify and favoured the proliferation of new evolving deep-water lineages among planktonic foraminifera.

This interpretation is also consistent with results obtained from stable isotope data on planktonic foraminiferal species at the Exmouth Plateau (Falzoni *et al.*, 2016). Data from Hole 762C reflect a habitat invasion by the more generalist *Marginotruncana* specimens that, starting in the late Coniacian, progressively migrated to shallower/warmer waters. The migration of marginotruncanids upward in the water column during the Santonian parallels the diversification of *Globotruncana* and of the more oligotrophic multiserial (*Sigalia* and *Ventilabrella*) taxa that may have occupied the deeper ecological niches as they became available with the increasing vertical stratification of surface waters.

The magnitude of the foraminiferal radiation event across the Coniacian–Santonian boundary interval indicates that other broader causes may need to be invoked or at least included (for example, global temperature variations and/or deep water circulation) to fully explain the observations. All of the Late Cretaceous compilations of oxygen isotope data on benthic and planktonic foraminifera from low to high-latitudes clearly indicate a global cooling trend starting in the Turonian and a progressive increase in the 'equator to pole' temperature gradient of surface waters, which was intensified during the Campanian (Huber *et al.*, 1995, 2002; Clarke & Jenkyns, 1999; Pucéat *et al.*, 2003; Friedrich *et al.*, 2012; Ando *et al.*, 2013; Falzoni *et al.*, 2013; Linnert *et al.*, 2014). Consequently, the development of a stable surface water circulation with a less fluctuating thermocline and well-defined upwelling and downwelling sites may have contributed to marine diversification and to the radiation of the deeper dweller taxa.

In addition to surface water ocean circulation, sea-level fluctuations and global temperature variations, changes in deep-water circulation patterns may have played a significant role in the planktonic foraminiferal evolution. However, available neodymium isotopic data from fish debris from low to high latitudes in the Atlantic, Indian, and Pacific Oceans as well as in the Tethys (MacLeod *et al.*, 2008, 2011; Jiménez Berrocoso *et al.*, 2010b; Robinson *et al.*, 2010; Murphy & Thomas, 2012; Robinson & Vance, 2012; Voigt *et al.*, 2013; Moiroud *et al.*, 2013) do not show any direct correlation with the planktonic foraminifera radiation event observed at the Coniacian/Santonian boundary. Further detailed studies on stratigraphically complete sections are needed to compare proxies for ocean circulation (for example, Nd isotopes) and planktonic foraminiferal ecological, evolutionary and compositional data.

CONCLUSIONS

This detailed documentation of foraminiferal species content and abundance across a continuous late Coniacian–early Santonian sequence drilled in Tanzania allow identification of the Coniacian/Santonian boundary by comparing the sequence of microfossil events with those observed at the GSSP for the base of the Santonian (Cantera de Margas section, Olazagutia, northern Spain). The implication is that, because of the absence of the inoceramid *Cladoceramus undulatoplicatus*, whose first appearance marks the base of the Santonian in the GSSP, the Coniacian/Santonian boundary in Tanzania is placed at the lowest occurrence of the GSSP secondary marker event *G. linneiana*. The authors note the difficulty in identifying the chemostratigraphic tie-points (Michel Dean and Kingsdown events) recorded in the GSSP type section and elsewhere.

Moreover, the Tanzanian record permits investigation of the evolution of planktonic foraminifera in a marginal depositional setting during a phase of sea-level transgression in which the effect of the epicontinental invasion of blue waters can be tested. The observed lithological and geochemical features of the sedimentary sequence reflect deposition in a subtropical marginal sea environment that evolved from an outer shelf to a slope setting with progressive reduction of the continental input, increase in seawater carbonate production and increase in water mass depth and vertical stratification of the ocean surface waters over coastal Tanzania. At Tanzania Drilling Project (TDP) Site 39 the environmental changes in the water column, as detected by the change in lithologies from the Lindi Formation to the Nangurukuru Formation coupled with variations in $\%CaCO_3$, $\%C_{org}$, $\delta^{13}C_{carb}$ and $\delta^{18}O_{carb}$, parallel the planktonic foraminifera assemblage evolution that resulted in a major compositional change with increased diversification and radiation of the deeper dwelling taxa.

It is hypothesized here that the correspondence between sedimentological and biological changes observed in Tanzania is linked to the invasion of oligotrophic water along the continental margin that may have provided increased opportunities for planktonic foraminifera to exploit new ecological niches and thus favoured the diversification of the more oligotrophic taxa. Although this scenario is consistent with the long-term high sea-level stand documented at a local and global scale, the evolution of planktonic foraminifera was certainly influenced by the combination of sea-level fluctuations, an increase in the ‘equator to pole’ temperature gradient, and changes in surface and deep-water ocean circulation

patterns. However, there remains a lack of adequate temporal constraints to unequivocally determine cause and effect relationships at a global scale.

ACKNOWLEDGEMENTS

We thank the Tanzania Petroleum Development Corporation, and particularly Joyce Singano, Emma Msaky, Frank Mayagilo and Uyubu for logistical support and the Tanzania Commission for Science and Technology for permission to drill. Thanks are extended to all the Tanzania Drilling Project team and especially to Jacqueline A. Lees, Amina K. Mweneinda, Helen Coxall and Heather Birch for fieldwork during the TDP 2009 drilling season. Insightful comments from two anonymous reviewers have greatly helped to improve this manuscript. Special thanks to Danuta Peryt for advice on the neoflabellinids. Thanks also to the Chief Editor, Tracy Frank, and the Associate Editor of this manuscript, Stuart A. Robinson, for guiding the review process. This research was funded by the DFG grant WE 4587/1-1, National Science Foundation (NSF EAR 0641956) to KMG and BTH and by the Smithsonian Institution's Charles Walcott Fund. Financial support to MRP and FF was provided by PUR 2008 (Università degli Studi di Milano). AJB was partly funded by Jacqueline A. Lees during fieldwork in Tanzania. The authors have no conflict of interest to declare regarding this work.

REFERENCES

Abramovich, S., Keller, G., Stüben, D. and **Berner, Z.** (2003) Characterization of late Campanian and Maastrichtian planktonic foraminiferal depth habitats and vital activities based on stable isotopes. *Palaeogeogr. Palaeoclimatol. Palaeoecol.*, **202**, 1–29.

Allan, J.R. and **Matthews, R.K.** (1982) Isotope signatures associated with early meteoric diagenesis. *Sedimentology*, **29**, 797–817.

Ando, A. and **Huber, B.T.** (2007) Taxonomic revision of the late Cenomanian planktonic foraminifera *Rotalipora greenhornensis* (Morrow, 1934). *J. Foramin. Res.*, **37**, 160–74.

Ando, A., Huber, B.T. and **MacLeod, K.G.** (2010) Depth-habitat reorganization of planktonic foraminifera across the Albian/Cenomanian boundary. *Paleobiology*, **36**, 357–373.

Ando, A., Woodard, S.C., Evans, H.F., Littler, K., Herrmann, S., MacLeod, K.G., Kim, S., Khim, B.-K., Robinson, S.A. and **Huber, B.T.** (2013) An emerging palaeoceanographic 'missing link': Multidisciplinary study of rarely recovered parts of deep-sea Santonian–Campanian transition from Shatsky Rise. *J. Geol. Soc. London*, **170**, 381–384.

Arthur, M.A. and **Schlanger, S.O.** (1979) Cretaceous "oceanic anoxic events" as causal factors in development of reef-reservoired giant oil fields. *Am. Assoc. Petr. Geol. B.,* **63**, 870–885.

Balduzzi, A., Msaky, E., Trincianti, E. and **Manum, S.B.** (1992) Mesozoic Karoo and post-Karoo Formations in the Kilwa area, southeastern Tanzania – a stratigraphic study based on palynology, micropalaeontology and well log data from the Kizimbani Well. *J. Afr. Earth Sc.,* **15**, 405–427.

Belford, D.J. (1983) A probably Coniacian (Late Cretaceous) foraminiferal fauna, Carnarvon Basin, western Australia. *Bull. Bur. Mineral Resour. Geol. Geophys.,* **217**, 11–27.

Bice, K.L., Huber, B.T. and **Norris, R.D.** (2003) Extreme polar warmth during the Cretaceous greenhouse? Paradox of the late Turonian $\delta^{18}O$ record at Deep Sea Drilling Project Site 511. *Paleoceanography*, **18**, 91–97.

Bornemann, A. and **Norris, R.D.** (2007) Size-related stable isotope changes in Late Cretaceous planktic foraminifera: Implications for paleoecology and photosymbiosis. *Mar. Micropaleontol.,* **65**, 32–42.

Bornemann, A., Norris, R.D., Friedrich, O., Beckmann, B., Schouten, S., Sinninghe Damsté, J.S., Vogel, J., Hofmann P. and **Wagner, T.** (2008) Isotopic evidence for glaciation during the Cretaceous Supergreenhouse. *Science*, **319**, 189–192.

Bush, A.B.G. and **Philander, G.H.** (1997) The Late Cretaceous: Simulation with a coupled atmosphere-ocean general circulation model. *Paleoceanography*, **12**, 595–516.

Caron, M. and **Homewood, P.** (1983) Evolution of early planktic foraminifers. *Mar. Micropaleontol.,* **7**, 453–462.

Clarke, L.J. and **Jenkyns, H.C.** (1999) New oxygen isotope evidence for long-term Cretaceous climatic change in the Southern Hemisphere. *Geology*, **27**, 699–702.

Coccioni, R. and **Premoli Silva I.** (2015) Revised Upper Albian–Maastrichtian planktonic foraminiferal biostratigraphy and magnetostratigraphy of the classical Tethyan Gubbio section (Italy). *Newslett. Stratigr*., **48**, 47–90.

Ernst, G. and **Zander, J.** (1993) Stratigraphy, facies development, and trace fossils of the Upper Cretaceous of southern Tanzania (Kilwa District). In: Geology and Mineral resources of Somalia and surrounding areas, Inst. Agron. Oltremare Firenze, Relaz. E. Monogr., **113**, 259–278.

Falzoni, F. and **Petrizzo, M.R.** (2011) Taxonomic overview and evolutionary history of *Globotruncanita insignis* (Gandolfi, 1955). *J. Foramin. Res.*, **41**, 371–383.

Falzoni, F., Petrizzo, M.R., MacLeod, K.G. and **Huber, B.T.** (2013) Santonian–Campanian planktonic foraminifera from Tanzania, Shatsky Rise and Exmouth Plateau: species depth ecology and paleoceanographic inferences. *Mar. Micropaleontol.*, **103**, 15–29.

Falzoni, F., Petrizzo, M.R., Huber, B.T. and **MacLeod, K.G.** (2014) Insights into the meridional ornamentation of the planktonic foraminiferal genus *Rugoglobigerina* (Late Cretaceous) and implications for taxonomy. *Cretaceous Res.*, **47**, 87–104.

Falzoni, F., Petrizzo, M.R., Clarke, L.C., MacLeod, K.G. and **Jenkyns, H.J.** (2016) Long-term Late Cretaceous carbon- and oxygen-isotope trends and planktonic foraminiferal turnover: a new record from the southern mid-latitudes. *GSA Bulletin*. doi: 10.1130/B31399.1

Forster, A., Schouten, S., Baas, M. and **Sinninghe Damsté, J.S.** (2007) Mid-Cretaceous (Albian–Santonian) sea surface temperature record of the tropical Atlantic Ocean. *Geology*, **35**, 919–922.

Frank, T.D., Thomas, D.J., Leckie, R.M., Arthur, M.A., Bown, P.R., Jones, K. and **Lees, J.A.** (2005) The Maastrichtian record from Shatsky Rise (northwest Pacific): A tropical perspective on global ecological and oceanographic changes. *Paleoceanography*, **20**. http://dx.doi.org/10.1029/2004PA001052 (PA1008).

Friedrich, O., Norris, R.D. and **Erbacher, J.** (2012) Evolution of middle to Late Cretaceous oceans–A 55 m.y. record of Earth's temperature and carbon cycle. *Geology*, **40**, 107–110.

Gale, A.S., Kennedy, W.J., Lees, J.A., Petrizzo, M.R. and **Walaszczyk, I.** (2007) An integrated study (inoceramid bivalves, ammonites, calcareous nannofossils, planktonic foraminifera, stable carbon isotopes) of the Ten Mile Creek section, Lancaster, Dallas County, north Texas, a candidate Global boundary Stratotype, Section and Point for the base of the Santonian Stage. *Acta Geol. Pol.*, **57**, 113–160.

Gale, A.S., Hancock, J.M., Kennedy, W.J., Petrizzo, M.R., Lees, J.A., Walaszczyk, I. and **Wray, D.S.** (2008) An integrated study (geochemistry, stable oxygen and carbon isotopes, nannofossils, planktonic foraminifera, inoceramid bivalves, ammonites and crinoids) of the Waxahachie Dam Spillway section, north Texas: a possible boundary stratotype for the base of the Campanian Stage. *Cretaceous Res.,* **29**, 131–167.

Gallemı, J., Lopez, G., Martınez, R. and **Pons, J.M.** (2007) Macrofauna of the Cantera de Margas section, Olazagutia: Coniacian/Santonian boundary, Navarro-Cantabrian Basin, northern Spain. *Cretaceous Res.,* **28**, 5–17.

Georgescu, M.D. and **Abramovich, S.** (2008) Taxonomic revision and phylogenetic classification of the Late Cretaceous (upper Santonian-Maastrichtian) serial planktonic foraminifera (Family Heterohelicidae Cushman, 1927) with peripheral test wall flexure. *Rev. Esp. Micropaleontol.,* **40**, 97–114.

Georgescu, M.D. and **Huber, B.T.** (2009) Early evolution of the Cretaceous serial planktonic foraminifera (late Albian–Cenomanian). *J. Foramin.Res.*, **39**, 335–360.

Giorgioni, M., Weissert, H., Bernasconi, S.M., Hochuli, P.A., Keller, C.E., Coccioni, R., Petrizzo, M.R., Lukeneder, A. and **Garcia, T.I.** (2015) Paleoceanographic changes during the Albian–Cenomanian in the Tethys and North Atlantic and the onset of the Cretaceous chalk. *Global Planet. Change*, **126**, 46–61.

Gonzalez-Donoso, J.-M., Linares, D. and **Robaszynski, F.** (2007) The rotaliporids, a polyphyletic group of Albian-Cenomanian planktonic foraminifera: emendation of genera. *J. Foramin. Res.*, **37**, 175–186.

Haq, B.U. (2014) Cretaceous eustasy revisited. *Global Planet. Change*, **113**, 44–58.

Hart, M.B. and **Bailey, H.W.** (1979) The distribution of planktonic Foraminiferida in the mid-Cretaceous of NW Europe. *Aspekte der kreide Europas*, **6**, 527–542.

Hart, M.B. (1980) A water depth model for the evolution of the planktonic Foraminiferida. *Nature*, **286**, 252–254.

Hart, M.B. (1999) The evolution and biodiversity of Cretaceous Foraminiferida. *Geobios*, **32**, 247–255.

Hay, W.W., Deconto, R., Wold, C.N., Wilson, K.M., Voigt, S., Schulz, M., Wold-Rossby, A., Dullo, W.C., Ronov, A.B., Balukhovsky, A.N. and **Soeding, E.** (1999) Alternative global Cretaceous paleogeography, in Barrera, E., Johnson, C.C., eds., The evolution of the Cretaceous ocean/climate system: Boulder, Colorado, Geological Society of America Special Paper, 332, 1–47.

Hay, W.W. (2008) Evolving ideas about the Cretaceous climate and ocean circulation. *Cretaceous Res.*, **29**, 725–753.

Hay, W.W. (2009). Cretaceous oceans and ocean modeling. *SEPM Special Publication*, **91**, 243–271.

Haynes, S.J., Huber, B.T. and **MacLeod, K.G.** (2015) Evolution and phylogeny of mid-Cretaceous (Albian–Coniacian) biserial planktic foraminifera. *J. Foramin. Res.*, **45**, 42–81.

Haynes, S.J., MacLeod, K.G., Huber, B.T., Warny, S., Kaufman, A.J., Pancost, R.D., Jiménez Berrocoso, Á., Petrizzo, M.R., Watkins, D. and **Zhelezinskaia, Y.** (2016, accepted) Depositional environments, marine and terrestrial links, and exceptional preservation in the Turonian of southeastern Tanzania. *GSA Bulletin*.

Herb, R. (1974) Cretaceous planktonic foraminifera from the Eastern Indian Ocean. Initial Reports of the Deep Sea Drilling Project 26, 745–770.

Huber, B.T. (1990) Maestrichtian planktonic foraminifer biostratigraphy of the Maud Rise (Weddell Sea, Antarctica): ODP Leg 113 Holes 689B and 690C. In: Barker, P. F., Kennett, *et al.*, (eds.), Proceedings of the Ocean Drilling Program, Scientific Results **113**. College Station, TX (Ocean Drilling Program), 489–513.

Huber, B.T. (1992) Paleobiogeography of Campanian-Maastrichtian foraminifera in the southern high latitudes. *Palaeogeogr. Palaeoclimatol. Palaeoecol.*, **92**, 325–360.

Huber, B.T., Hodell, D.A. and **Hamilton, C.P.** (1995) Middle-Late Cretaceous climate of the southern high latitudes: Stable isotopic evidence for minimal equator-to-pole thermal gradients. *Geol. Soc. Am. Bull.*, **107**, 1164–1191.

Huber, B.T., Leckie, R.M., Norris, R.D., Bralower, T.J. and **CoBabe, E.** (1999) Foraminiferal assemblage and stable isotopic change across the Cenomanian-Turonian boundary in the subtropical North Atlantic. *J. Foramin. Res.*, **29**, 392–417.

Huber, B.T., Norris, R.D. and **MacLeod, K.G.** (2002) Deep-sea paleotemperature record of extreme warmth during the Cretaceous. *Geology*, **30**, 123–126.

Huber, B.T. and **Leckie, R.M.** (2011) Planktic foraminiferal species turnover across deep-sea Aptian/Albian boundary sections. *J. Foramin. Res.*, **41**, 53–95.

Huber, B.T. and **Petrizzo, M.R.** (2014) Evolution and taxonomic study of the Cretaceous planktic foraminiferal genus *Helvetoglobotruncana* Reiss, 1957. *J. Foramin. Res.*, **44**, 40–57.

Jarvis, I., Gale, A.S., Jenkyns, H.C. and **Pearce, M.A.** (2006) Secular variation in Late Cretaceous carbon isotopes: a new $\delta^{13}C$ carbonate reference curve for the Cenomanian–Campanian (99.6–70.6 Ma). *Geol. Mag.*, **143**, 561–608.

Jenkyns, H.C. (1980) Cretaceous anoxic events: from continents to oceans. *J. Geol. Soc. London*, **137**, 171–188.

Jenkyns, H.C., Gale, A.S., and **Corfield, R.M.** (1994) Carbon- and oxygen-isotope stratigraphy of the English Chalk and Italian Scaglia and its palaeoclimatic significance. *Geol. Mag.*, **131**, 1–34.

Jiménez Berrocoso, Á., MacLeod, K.G., Huber, B.T., Lees, J.A., Wendler, I., Bown, P.R., Mweneinda, A.K., Isaza-Londoño, C. and **Singano, J.M.** (2010a) Lithostratigraphy, biostratigraphy and chemostratigraphy of Upper Cretaceous sediments from southern Tanzania: Tanzania Drilling Project sites 21-26. *J. Afr. Earth Sci.*, **57**, 47–69.

Jiménez Berrocoso, Á., MacLeod, K.G., Martin, E.E., Bourbon, E., Londoño, C. I. and **Basak, C.** (2010b) Nutrient trap for Late Cretaceous organic-rich black shales in the tropical North Atlantic. *Geology*, **38**, 1111–1114.

Jiménez Berrocoso, Á., Huber, B.T., MacLeod, K.G., Petrizzo, M.R., Lees, J.A., Wendler, I., Coxall, H., Mweneinda, A.K., Falzoni, F., Birch, H., Singano, J.M., Haynes, S., Cotton, L., Wendler, J., Bown, P.R., Robinson, S.A. and **Gould, J.** (2012) Lithostratigraphy, biostratigraphy and chemostratigraphy of Upper Cretaceous and Paleogene sediments from southern Tanzania: Tanzania Drilling Project Sites 27 to 35. *J. Afr. Earth Sci.*, **70**, 36–57.

Jiménez Berrocoso, Á., Elorza, J. and **MacLeod, K.G.** (2013) Proximate environmental forcing in fine-scale geochemical records of calcareous couplets (Upper Cretaceous and Palaeocene of the Basque-Cantabrian Basin, eastern North Atlantic). *Sed. Geol.*, **284-285**, 76–90.

Jiménez Berrocoso, Á., Huber, B.T., MacLeod, K.G., Petrizzo, M.R., Lees, J.A., Wendler, I., Coxall, H., Mweneinda, A.K., Falzoni, F., Birch, H., Haynes, S.J., Bown, P.R., Robinson, S.A. and **Singano, J.M.** (2015) Lithostratigraphy, biostratigraphy and chemostratigraphy of Upper Cretaceous and Paleogene sediments from southern Tanzania: Tanzania Drilling Project Sites 36 to 40. *J. Afr. Earth Sci.*, **101**, 282–308.

Kapilima, S. (2003) Tectonic sedimentary evolution of the coastal basin of Tanzania during the Mesozoic times. *Tanzania J. Sci.*, **29**, 1–16.

Kejato, H. (2003) The geology and petroleum potential of Tanzania. Tanzania Petroleum Development Corporation, Dar-es-Salaam.

Kennedy,W.J., Walaszczyk, I. and **Klinger, H.C.** (2008) *Cladoceramus* (Bivalvia, Inoceramidae) – ammonite associations from Kwa Zulu, South Africa. *Cretaceous Res.*, **29**, 267–293.

Kennedy,W.J. and **Klinger, H.C.** (2014) Cretaceous faunas from Zululand and Natal, South Africa. *Texasia cricki* Spath, 1921 (Cephalopoda: Ammonoidea) an early Santonian marker fossil from the Mzamba Formation of the Eastern Cape Province. *Palaeont. afr.*, **48,** 34–40.

Key, R.M., Smith, R.A., Smelor, M., Sæther, O.M., Thorsnes, T., Powell, J.H., Njange, F. and **Zandamela, E.B.** (2008) Revised lithostratigraphy of the Mesozoic-Cenozoic succession of the onshore Rovuma Basin, northern coastal Mozambique. *S. Afr. J. Geol.*, **111**, 89–108.

Kopaevich, L.F., Beniamovski, V.N. and **Sadekov, A.Yu.** (2007) Middle Coniacian – Santonian foraminiferal bioevents around the Mangyshlak Peninsula and Russian Platform. *Cretaceous Res.*, **28**, 108–118.

Krasheninnikov, V.A. and **Basov, I.A.** (1983) Stratigraphy of Cretaceous Sediments of the Falkland Plateau based on planktonic foraminifers, Deep-Sea Drilling Project, Leg 71. Initial Reports of the Deep Sea Drilling Project, **71**, 789–820.

Lamolda, M.A. and **Paul, C.R.C.** (2007) Carbon and oxygen stable isotopes across the Coniacian/Santonian boundary at Olazagutia, northern Spain. *Cretaceous Res.*, **28**, 37–45.

Lamolda, M.A. and **Paul, C.R.C.** (2009) Testing the precision of bioevents. *Geol. Mag.*, **146**, 625–637.

Lamolda, M.A., Paul, C.R.C., Peryt, D. and **Pons, J.M.** (2014) The Global Boundary Stratotype and Section Point (GSSP) for the base of the Santonian Stage, "Cantera de Margas", Olazagutia, northern Spain. *Episodes*, **37**, 1–13.

Leary, P.N. and **Hart, M.B.** (1989) The use of ontogeny of deep water dwelling planktic foraminifera to assess basin morphology, the development of water masses, eustasy and the position of the oxygen minimum zone in the water column. *Mesozoic Research*, **2**, 67–74.

Leckie, R.M. (1987) Paleoecology of mid-Cretaceous planktonic foraminifera: a comparison of open ocean and Epicontinental Sea assemblages. *Micropaleontology*, **33**, 164–176.

Leckie, R.M. (2009) Seeking a better life in the plankton. *Proc. Natl Acad. Sci.*, **106** (34), 14183–14184.

Linares Rodriguez, D. (1977) Foraminiferos plantònicos del Cretàcico superior de las Cordilleras Béticas (Sector central). Tesis Doctoral, Departamento de Geologia, Universidad de Malaga, 410 pp.

Linnert, C., Robinson, S.A., Lees, J.A., Bown, P.N., Pérez-Rodríguez, I., Petrizzo, M.R., Falzoni, F., Littler, K., Arz, J.A. and **Russell, E.E.** (2014) Evidence for global cooling in the Late Cretaceous. *Nature Communications*, **5**, 4194.

MacLeod, K.G., Huber, B.T., Pletsch, T., Röhl, U. and **Kucera, M.** (2001) Maastrichtian foraminiferal and paleoceanographic changes on Milankovitch time scales. *Paleoceanography*, **16**, 133–154.

MacLeod, K.G., Martin, E.E. and **Blair, S.W.** (2008) Nd isotopic excursion across Cretaceous ocean anoxic event 2 (Cenomanian-Turonian) in the tropical North Atlantic. *Geology*, **36**, 811–814.

MacLeod, K.G., Isaza Londoño, C., Martin, E.E., Jiménez Berrocoso, Á. and **Basak, C.** (2011) Nd evidence for changes in North Atlantic Circulation at the end of the Cretaceous greenhouse. *Nature Geoscience*, **4**, 779–782.

MacLeod, K.G., Huber, B.T., Jiménez Berrocoso, Á. and **Wendler, I.** (2013) A stable and hot Turonian without glacial $\delta^{18}O$ excursions is indicated by exquisitely preserved Tanzanian foraminifera. *Geology*, **41**, 1083–1086.

Melinte, M.C. and **Lamolda, M.A.** (2007) Calcareous nannofossil biostratigraphy of the Coniacian/Santonian boundary interval in Romania and comparison with other European regions. *Cretaceous Res.*, **28**, 119–127.

Moiroud, M., Pucéat, E., Donnadieu, Y., Bayon, G., Moriya, K., Deconinck, J.F. and **Boyet, M.** (2013) Evolution of the neodymium isotopic signature of neritic seawater on a northwestern Pacific margin: new constrains on possible end-members for the composition of deep-water masses in the Late Cretaceous ocean. *Chemical Geology*, **356**, 160–170.

Mpanda, S. (1997) Geological development of the East African coastal basin of Tanzania. *Stockholm Contrib. Geol.*, **45**, 1–127.

Murphy, D.P. and **Thomas, D.J.** (2012) Cretaceous deep‐water formation in the Indian sector of the Southern Ocean. *Paleoceanography*, **27**, PA1211.

Nederbragt, A.J. (1990) Biostratigraphy and paleoceanographic potential of the Cretaceous planktic foraminifera Heterohelicidae. *Centrale Huisdrukkerij Vrije Universiteit*, Amsterdam.

Nederbragt, A.J., Erlich, R.N., Fouke, B.W. and **Ganssen, G.M.** (1998) Palaeoecology of the biserial planktonic foraminifer *Heterohelix moremani* (Cushman) in the late Albian to middle Turonian circum-North Atlantic. *Palaeogeogr. Palaeoclimatol. Palaeoecol.*, **144**, 115–133.

Nicholas, C.J., Pearson, P.N., Bown, P.R., Dunkley Jones, T., Huber, B.T., Karega, A., Lees, J.A., McMillan, I.K., O'Halloran, A., Singano, J.M. and **Wade, B.S.** (2006) Stratigraphy and sedimentology of the Upper Cretaceous to Paleogene Kilwa Group, southern coastal Tanzania. *J. Afr. Earth Sci.*, **45**, 431–466.

Nicholas, C.J., Pearson, P.N., McMillan, I.K., Ditchfield, P.W. and **Singano, J.S.** (2007) Structural evolution of coastal Tanzania since the Jurassic. *J. Afr. Earth Sc.*, **48**, 273–297.

Norris, R.D. and **Wilson, P.A.** (1998) Low-latitude sea-surface temperatures for the mid-Cretaceous and the evolution of planktonic foraminifera. *Geology*, **26**, 823–826.

Norris, R.D., Bice, K.L., Magno, E.A. and **Wilson, P.A.** (2002) Jiggling the tropical thermostat in the Cretaceous hothouse. *Geology*, **30**, 299–302.

Olsson, R.K., Hemleben, C., Berggren, W.A. and **Huber, B.T.** (1999) Atlas of Paleocene Planktonic Foraminifera. *Smithsonian Contributions to Paleobiology*, **85**, 252 pp.

Otto-Bliesner, B.L., Brady, E.C. and **Shields, C.** (2002) Late Cretaceous ocean: Coupled simulations with the National Center for Atmospheric Research Climate System Model. *J. Geophys. Res.*, **107**, NO. D2, 4019,1.

Pearson, P.N., Nicholas, C.J., Singano, J.M., Bown, P.R., Coxall, H.K., van Dongen, B.E., Huber, B.T., Karega, A., Lees, J.A., Msaky, E., Pancost, R.D., Pearson, M. and **Roberts, A.P.** (2004) Paleogene and Cretaceous sediment cores from the Kilwa and Lindi areas of coastal Tanzania: Tanzania Drilling Project Sites 1–5. *J. Afr. Earth Sc.*, **39**, 25–62.

Pearson, P.N., Olsson, R.K., Huber, B.T., Hemleben, C. and **Berggren, W.A.** (2006) Atlas of Eocene Planktonic foraminifera. *Cushman Foundation Special Publication*, **41**, 513 pp.

Peryt, D. and **Lamolda, M.A.** (2007) Neoflabellinids (benthic foraminifers) from the Upper Coniacian and Lower Santonian at Olazagutia, Navarra province, Spain; taxonomy and correlation potential. *Cretaceous Res.*, **21**, 30–36.

Petrizzo, M.R. (2000) Upper Turonian-lower Campanian planktonic foraminifera from southern mid-high latitudes (Exmouth Plateau, NW Australia): biostratigraphy and taxonomic notes. *Cretaceous Res.*, **21**, 479–505.

Petrizzo, M.R. and **Premoli Silva, I.** (2000) Upper Cretaceous meridionally costellate hedbergellids: the genus *Meridionalla* El-Nakhal, 1982 vs. the genus *Costellagerina* Petters, El-Nakhal and Cifelli, 1983. *J. Foramin. Res.*, **30**, 306–309.

Petrizzo, M.R. (2001) Late Cretaceous planktonic foraminifera from Kerguelen Plateau (ODP Leg 183): new data to improve the Southern Ocean biozonation. *Cretaceous Res.*, **22**, 829–855.

Petrizzo, M.R. (2002) Palaeoceanographic and palaeoclimatic inferences from Late Cretaceous planktonic foraminiferal assemblages from the Exmouth Plateau (ODP Sites 762 and 763, eastern Indian Ocean). *Mar. Micropaleontol.*, **45**, 117–150.

Petrizzo, M.R. (2003) Late Cretaceous planktonic foraminiferal bioevents in the Tethys and in the Southern Ocean record: an overview. *J. Foramin. Res.*, **33**, 330–337.

Petrizzo, M.R. and **Huber, B.T.** (2006a) Biostratigraphy and taxonomy of Late Albian planktonic foraminifera from ODP Leg 171b (western north Atlantic Ocean). *J. Foramin. Res.*, **36**, 165–189.

Petrizzo, M.R. and **Huber, B.T.** (2006b) On the phylogeny of the late Albian genus *Planomalina*. *J. Foramin. Res.*, **36**, 233–240.

Petrizzo, M.R., Huber, B.T., Wilson, P.A. and **MacLeod, K.G.** (2008) Late Albian paleoceanography of the western subtropical North Atlantic. *Paleoceanography*, **23**, PA1213.

Petrizzo, M.R., Falzoni, F. and **Premoli Silva, I.** (2011) Identification of the base of the lower-to-middle Campanian *Globotruncana ventricosa* Zone: comments on reliability and global correlations. *Cretaceous Res.*, **32**, 387–405.

Petrizzo, M.R., Caron, M. and **Premoli Silva, I.** (2015) Remarks on the identification of the Albian/Cenomanian boundary and taxonomic clarification of the planktonic foraminifera index species *globotruncanoides*, *brotzeni* and *tehamaensis*. *Geol. Mag.*, **152**, 521–536.

Postuma J.A. (1971) Manual of planktonic foraminifera. Elsevier, Amsterdam, 420 pp.

Poulsen, C.J., Seidov, D., Barron, E.J. and **Peterson, W.H.** (1998) The impact of paleogeographic evolution on the surface oceanic. *Paleoceanography*, **13**, 546–559.

Premoli Silva, I. and **Sliter, W.V.** (1995) Cretaceous planktonic foraminiferal biostratigraphy and evolutionary trends from the Bottaccione section, Gubbio, Italy. *Palaeontographia Italica*, **81**, 2–90.

Premoli Silva, I. and **Sliter, W.V.** (1999) Cretaceous paleoceanography: evidence from planktonic foraminiferal evolution. In: Barrera, E., Johnson, C.C., (Eds.), The Evolution of the Cretaceous Ocean-Climate System. *Special Papers of the Geological Society of America*, **332**, 301–328.

Price, G.D., Sellwood, B.W., Corfield, R.M., Clarke, L. and **Cartlidge, J.E.** (1998) Isotopic evidence for paleotemperatures and depth stratification of middle Cretaceous planktonic foraminifera from the Pacific Ocean. *Geol. Mag.*, **135**, 183–191.

Pucéat, E., Lécuyer, C., Sheppard, S. M., Dromart, G., Reboulet, S. and **Grandjean, P.** (2003) Thermal evolution of Cretaceous Tethyan marine waters inferred from oxygen isotope composition of fish tooth enamels. *Paleoceanography*, **18**, PA000823.

Pucéat, E., Lécuyer, C. and **Reisberg, L.** (2005) Neodymium isotope evolution of NW Tethyan upper ocean waters throughout the Cretaceous. *Earth Planet. Sci. Lett.*, **236**, 705–720.

Ryan, W.B.F. and **Cita, M.B.** (1977) Ignorance concerning episodes of ocean-wide stagnation. *Mar. Geol.*, **23**, 197–215.

Robaszynski, F., Caron, M., and the European Working Group on Planktonic Foraminifera (1979) Atlas of mid Cretaceous planktonic foraminifera (Boreal Sea and Tethys), C.N.R.S. Paris, France. *Cah. Micropaléontol.*, **1, 2**.

Robaszynski, F., Caron, M., Gonzalez-Donoso, J.M., Wonders, A.H. and the European Working Group on Planktonic Foraminifera (1984) Atlas of Late Cretaceous Globotruncanids. *Rev. Micropaléontol.*, **26**, 145–305.

Robaszynski, F. and **Caron, M.** (1995) Foraminiféres planctoniques du Crétacé: commentaire de la zonation Europe-Méditerranée. *Bull. Soc. Géol. Fr.*, **166**, 681–692.

Robaszynski, F., Gonzalez Donoso, J.M., Linares, D., Amédro, F., Caron, M., Dupuis, C., Dhondt, A.V. and **Gartner, S.** (2000) Le Crétacé supérieur de la région de Kalaat Senan, Tunisie Centrale. Litho-biostratigraphie intégrée: zones d'ammonites, de foraminifères planctoniques et de nannofossiles du Turonien supérieur au Maastrichtien. *Bull. Centres Rech Explor.-Prod. Elf-Aquitaine*, **22**, 359–490.

Robinson, S.A., Murphy, D.P., Vance, D. and **Thomas, D.J.** (2010) Formation of "Southern Component Water" in the Late Cretaceous: Evidence from Nd-isotopes. *Geology*, **38**, 871–874.

Robinson, S.A. and **Vance, D.** (2012) Widespread and synchronous change in deep-ocean circulation in the North and South Atlantic during the Late Cretaceous: *Paleoceanography*, **27**, PA1102.

Salaj, J. (1984) Boundaries of the Upper Cretaceous hypostratotypes at the profile Djebel Fguria Salah, Tunisia. *Bull. Geol. Soc. Denmark*, **33**, 199–201.

Salman, G., and **Abdula, I.** (1995) Development of the Mozambique and Ruvuma sedimentary basins, offshore Mozambique. *Sed. Geol.*, **96**, 7–41.

Schlanger, S.O. and **Jenkyns, H.C.** (1976) Cretaceous oceanic anoxic events; causes and consequences. *Geologie en Mijnbouw*, **55**, 179–184.

Sliter, W.V. (1977) Cretaceous foraminifers from the southwestern Atlantic Ocean, Leg 36, Deep Sea Drilling Project. In: Barker, P. F., Dalziel, I. W. D. *et al.*, (eds.), Initial Reports of the Deep Sea Drilling Project 36. U.S. Government Printing Office, Washington, D.C., 519–573.

Sliter, W.V. (1992) Cretaceous planktonic foraminiferal biostratigraphy and paleoceanographic events in the Pacific Ocean with emphasis on indurated sediment. *Centenary of Japanese Micropaleontology*. Terra Scientific Publishing Company, Tokyo, 281–299.

Soldan, D.M., Petrizzo, M.R., Premoli Silva, I. and **Cau A.** (2011) Phylogenetic relationships and evolutionary history of the Paleogene genus *Igorina* through parsimony analysis. *J. Foramin. Res.*, **41**, 260–284.

Soldan, D.M., Petrizzo, M.R. and **Premoli Silva, I.** (2014) *Pearsonites* nov. gen. a new Paleogene planktonic foraminifera genus name for the *broedermanni* lineage. *J. Foramin. Res.*, **44**, 17–27.

Sprovieri, M., Sabatino, N., Pelosi, N., Batenburg, S.J., Coccioni, R., Iavarone, M. and **Mazzola, S.** (2013) Late Cretaceous orbitally-paced carbon isotope stratigraphy from the Bottaccione Gorge (Italy). *Palaeogeogr. Palaeoclimatol. Palaeoecol.*, **379**, 81–94.

Steinhauff, D.M., Walker, K. and **Goldberg, S.** (1999) Diagenesis by burial fluids, middle Ordovician platform to platform-margin limestones, East Tennessee: relationship to Mississippi Valley-type deposits. *J. Sed. Res.*, **69**, 1107–1122.

Takashima, R., Nishi, H., Yamanaka, T., Hayashi, K., Waseda, A., Obuse, A., Tomosugi, T., Deguchi, N. and **Mochizuki, S.** (2010) High-resolution terrestrial carbon

isotope and planktic foraminiferal records of the Upper Cenomanian to the Lower Campanian in the Northwest Pacific. *Earth Planet. Sci. Lett.*, **289**, 570–582.

Veeken, P.C.H. and **Titov, K.V.** (1996) Gravity modelling along a seismic line across the Mandawa basin, southeastern Tanzania. *J. Afr. Earth Sc.*, **22**, 207–217.

Voigt, S., Friedrich, O., Norris, R.D. and **Schönfeld, J.** (2010) Campanian – Maastrichtian carbon isotope stratigraphy: shelf-ocean correlation between the European shelf sea and the tropical Pacific Ocean. *Newslett. Stratigr.*, **44**, 57–72.

Voigt, S., Jung, C., Friedrich, O., Frank, M., Teschner, C. and **Hoffmann, J.** (2013) Tectonically restricted deep-ocean circulation at the end of the Cretaceous greenhouse. *Earth Planet. Sci. Lett.*, **369-370**, 169–177.

Wagreich, M. (2009) Coniacian-Santonian oceanic red beds and their link to Oceanic Anoxic Event 3, in: Cretaceous Oceanic Red Beds: Stratigraphy, Composition, Origins, and Paleoceanographic and Paleoclimatic Significance, edited by: Hu, X.,Wang, C., Scott, R.W., Wagreich, M. and Jansa, L.. *SEPM Spec. P.*, **91**, 235–242.

Wagreich, M. (2012) "OAE 3" – regional Atlantic organic carbon burial during the Coniacian–Santonian. *Clim. Past*, **8**, 1447–1455.

Walaszczyk, I., Kopaevich, L.F. and **Beniamovski, V.N.** (2013) Inoceramid and foraminiferal record and biozonation of the Turonian and Coniacian (Upper Cretaceous) of the Mangyshlak Mts., western Kazakhstan. *Acta Geol. Pol.*, **63**, 469–487.

Walaszczyk, I., Kennedy W.J., Dembicz, K., Gale, A.S., Praszkier, T., Rasoamiaramanana, A.H. and **Randrianaly, H.** (2014) Ammonite and inoceramid biostratigraphy and biogeography of the Cenomanian through basal Middle Campanian (Upper Cretaceous) of the Morondava Basin, western Madagascar. *J. Afr. Earth Sci.*, **89**, 79–132.

Wendler, I., Wendler, J., Gräfe, K.-U., Lehmann, J. and **Willems, H.** (2009) Turonian to Santonian carbon isotope data from the Tethys Himalaya, southern Tibet. *Cretaceous Res.*, **30**, 961–979.

Wendler, I., Huber, B.T., MacLeod, K.G. and **Wendler, J.E.** (2013) Stable oxygen and carbon isotope systematics of exquisitely preserved Turonian foraminifera from Tanzania – understanding isotopic signatures in fossils. *Mar. Micropaleontol.*, **102**, 1–33.

Wendler, I. (2013) A critical evaluation of carbon isotope stratigraphy and biostratigraphic implications for Late Cretaceous global correlation. *Earth-Sci. Rev.*, **126**, 116–146.

Wendler, J.E. and **Bown, P.R.** (2013) Exceptionally well-preserved Cretaceous microfossils reveal new biomineralization styles. *Nature Communication*, **4**. http://dx.doi.org/10.1038/ncomms3052.

Wilson, P.A., Norris, R.D. and **Cooper, M.J.** (2002) Testing the Cretaceous greenhouse hypothesis using glassy foraminiferal calcite from the core of the Turonian tropics on Demerara Rise. *Geology*, **30**, 607–610.

Wonders, A.A.H. (1980) Middle and Late Cretaceous planktonic foraminifera of the western Mediterranean area. *Utrecht Micropaleontol. Bull.*, **24**, 1–158.

Wonders, A.A.H. (1992) Cretaceous planktonic foraminiferal biostratigraphy, Leg 122, Exmouth Plateau, Australia. Proceedings of the Ocean Drilling Program, Scientific Results **122**. College Station, TX (Ocean Drilling Program), 587–599.

SUPPORTING INFORMATION

SI – Table 1. Geochemical data.

SI – Table 2. Distribution chart of planktonic foraminifera

SI – Taxonomic notes.

CAPTIONS

Fig. 1. Location of TDP Site 39 in south-east coastal Tanzania.

Fig. 2. Outcrop of the Coniacian–Santonian sediments along the roadside north of Nangurukuru Junction (GPS = 8°45’ 0.97” S, 39°17’ 62.6” E, elevation 45 m).

Fig. 3. Lithostratigraphy, planktonic foraminiferal biostratigraphy and age of Tanzania Drilling Project (TDP) Site 39. Nannofossil zones from Jiménez Berrocoso *et al.* (2015). (A) Well-lithified, massive, silty claystones from the Lindi Formation (core 36). (B) Finely laminated fabrics from the Lindi Formation at core 40. (C) Core 26 showing alternating dark and light intervals of the Nangurukuru Formation. Note a sharp boundary at 1.88 cm between a dark interval (uppermost part the core) and a lighter interval (middle sector of the core). A gradational boundary, however, is appreciated at *ca* 1.54 cm between the lighter interval (middle sector of the core) and a dark interval (lowermost part of the core). (D) Detail view of core 14 (Nangurukuru Formation) that shows abundant burrows in dark grey, calcareous, clayey siltstones. (E) Detail view of core 9 (calcareous, clayey siltstones; Nangurukuru Formation). The reddish colour (oxide stain) of the core (upper half of the picture) is due to modern subtropical weathering. (F) Thin layers of white-coloured, carbonate-cemented siltstones (core 14; Nangurukuru Formation). Ruler scale in core photographs (A) to (F) is in centimetres.

Fig. 4. Foraminiferal bioevents at Tanzania Drilling Project (TDP) Site 39. Lithostratigraphy legend, biozonations and age as in Fig. 3.

Fig. 5. Lithostratigraphy, biostratigraphy and chemostratigraphy of Tanzania Drilling Project (TDP) Site 39. Black symbols = lithologies are dark grey to black in colour; grey symbols = lithologies are light grey in colour. Intervals 1 to 5 of the $\delta^{13}C_{carb}$ curve are explained in the text. Lithostratigraphy legend, biozonations and age as in Fig. 3.

Fig. 6. Chemostratigraphic and biostratigraphic events at the GSSP section (Cantera de Margas quarry section, Olazagutia, Basque–Cantabrian Region, northern Spain) for defining the base of the Santonian Stage (compilation based on data in Lamolda *et al.*, 2014, and references therein).

Fig. 7. (A) Comparison of the $\delta^{13}C$ curves at Tanzania Drilling Project (TDP) Site 39 and Cantera de Margas section. (B) Graphic correlation of the common microfossil bioevents between TDP Site 39 and the Cantera de Margas section. Nannofossil bioevents from TDP Site 39 are from Jiménez Berrocoso *et al.* (2015). A best-fit regression curve is applied. LO = lowest occurrence; HO = highest occurrence. See text for further explanations.

Fig. 8. Planktonic foraminiferal percent abundance plotted relative to the total foraminifera. Planktonic foraminifera genera and species richness, evolutionary rates, stratigraphic distribution of selected genera and percent abundance of the genera plotted relative to the total planktonic foraminiferal assemblages at Tanzania Drilling Project (TDP) Site 39. Intervals of planktonic foraminiferal faunal changes (1 and 2), ecological intervals (A, B and C) are according to the text.

Fig. 9. SEM images of foraminiferal species. Scale bars 200 μm. 1a to 1c, *Marginotruncana tarfayensis* (TDP 39/29-3, 1 to 25 cm); 2a to 2c, *Marginotruncana schneegansi* (TDP 39/28-1, 1-25 cm); 3a to 3c, *Marginotruncana coronata* (TDP 39/29-3, 1 to 25 cm); 4a to 4c, *Marginotruncana pseudolinneiana* (TDP 39/30-2, 1 to 25 cm); 5a to 5c, *Globotruncana linneiana* (TDP 39/9-1, 25 to 56 cm); 6a to 6c, *Marginotruncana sinuosa* (TDP 39/19-2, 1 to 25 cm); 7a to 7c; *Contusotruncana morozovae* (TDP 39/9-1, 25 to 56 cm); 8a to 8c, *Marginotruncana angusticarenata* (TDP 39/29-3, 1 to 25 cm)*;* 9a to 9c, *Contusotruncana fornicata* (TDP 39/19-1, 1 to 17 cm)*;* 10a to 10b, *Planoheterohelix praenuttalli* (TDP 39/28-1, 1 to 25 cm); 11a to 11b, *Pseudotextularia nuttalli* (TDP 39/31-1, 1 to 25 cm).

Fig. 10. SEM images of foraminiferal species. Scale bars 200 μm except where otherwise stated. 1a to 1c, *Marginotruncana pseudomarginata* (TDP 39/32-3, 1 to 25 cm); 2a to 2c, *Dicarinella marginata* (TDP 39/16-1, 1 to 24 cm); 3a to 3c, *Globotruncanita elevata* (TDP 39/16-2, 1 to 25 cm); 4a to 4c, *Dicarinella concavata* (TDP 39/29-3, 1 to 25 cm); 5a to 5c, *Marginotruncana undulata* (TDP 39/29-2, 1 to 25 cm), scale bar 500 μm; 6a to 6c, *Dicarinella asymetrica* (TDP 39/16-1, 1 to 24 cm); 7a to 7c, *Dicarinella imbricata* (TDP 39/37-2, 91 to 110 cm); 8a to 8c, *Globotruncanita elevata* (TDP 39/2-1, 1 to 25 cm), scale bar 500 μm; 9a to 9c, *Dicarinella imbricata* (TDP 39/27-3, 1 to 25 cm); 10a to 10c, *Dicarinella canaliculata* (TDP 39/30-3, 1 to 25 cm).

Fig. 11. SEM images of foraminiferal species. Scale bars 200 μm except where otherwise stated. 1a to 1c, *Whiteinella archaeocretacea* (TDP 39/16-1, 1 to 24 cm); 2a-c, *Muricohedbergella flandrini* (TDP 39/16-1, 25 to 60 cm); 3a to 3c, *Costellagerina pilula* (TDP 39/11-1, 25 to 54 cm), scale bar 100 μm; 4a to 4c, '*Muricohedbergella' simplex* (TDP 39/27-3, 1 to 25 cm); 5a to 5b, *Sigalia carpatica* (TDP 39/11-1, 1 to 25 cm); 6a to 6b, *Sigalia decoratissima* (TDP 39/10-2, 47 to 70 cm); 7a-b, *Ventilabrella eggeri* (TDP 39/9-1, 25 to 46 cm); 8a to 8b, '*Heterohelix' sphenoides* (TDP 39/9-1, 25 to 46 cm); 9a to 9b, *Planoheterohelix moremani* (TDP 39/9-1, 25 to 26 cm), scale bar 100 μm; 10a to 10b,

Neoflabellina gibbera (TDP 39/8-1, 24 to 55 cm); 11a to 11b, *Huberella huberi* (TDP 39/35-2, 1 to 25 cm), scale bar 100 μm; 12a to 12b, *Ventilabrella glabrata* (TDP 39/2-1, 1 to 25 cm); 13a to 13b, '*Heterohelix' papula* (TDP 39/10-2, 47 to 70 cm), scale bar 100 μm; 14a to 14c, '*Heterohelix' papula* (TDP 39/12-1, 1 to 25 cm), a to b, scale bar 100 μm; c, scale bar 20 μm.

Fig. 12. SEM images of foraminiferal species. Scale bars 100 μm. 1a to 1c, *Globotruncana arca* (TDP 39/4-1, 17 to 40 cm); 2a to 2c, *Whiteinella brittonensis* (TDP 39/20-1, 1 to 27 cm); 3a to 3c, *Whiteinella brittonensis* (TDP 39/20-2, 1 to 31 cm); 4a to 4c, *Whiteinella aprica* (TDP 39/20-1, 1 to 27 cm); 5a to 5c *Whiteinella aprica* (TDP 39/19-1, 1 to 17 cm); 6a to 6c, *Whiteinella aumalensis* (TDP 39/19-1, 1 to 17 cm); 7a to 7b, *Globigerinelloides alvarezi* (TDP 39/39-1, 1 to 25 cm); 8a to 8b, *Globigerinelloides ehrenbergi* (TDP 39/12-1, 1 to 25 cm); 9a to 9b, *Globigerinelloides praevolutus* (TDP 39/33-2, 1 to 25 cm); 10a to 10b, *Globigerinelloides prairiehillensis* (TDP 39/22-2, 1 to 26 cm); 11a to 11b, *Globigerinelloides yaucoensis* (TDP 39/15-1, 26 to 50 cm); 12a to 12b, *Globigerinelloides bollii* (TDP 39/10-1, 25 to 56 cm).

Fig. 13. *Dicarinella asymetrica* evolutionary lineage. Percent abundance of *Dicarinella concavata*, *D. asymetrica* and transitional forms at Tanzania Drilling Project (TDP) Site 39 plotted relative to the total planktonic foraminiferal assemblages. Stars indicate the occurrence level of single-keeled *D. asymetrica* specimens.

Fig. 14. *Globotruncanita elevata* evolutionary lineage. Percent abundance of *Marginotruncana undulata*, *Marginotruncana* cf. *undulata*, *Globotruncanita stuartiformis* and *Globotruncanita elevata* at Tanzania Drilling Project (TDP) Site 39 plotted relative to the total planktonic foraminiferal assemblages.

Fig. 15. Palaeoceanographic scenario inferred for coastal Tanzania according to the lithological, geochemical and planktonic foraminiferal changes. See text for explanations.

Fig. 1

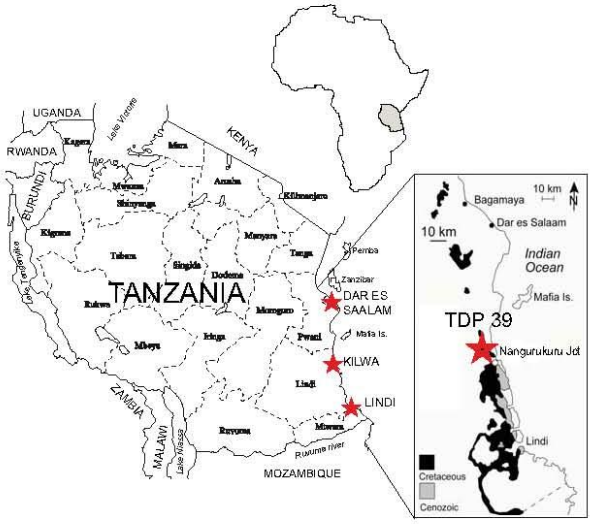

Fig. 2

Fig. 3

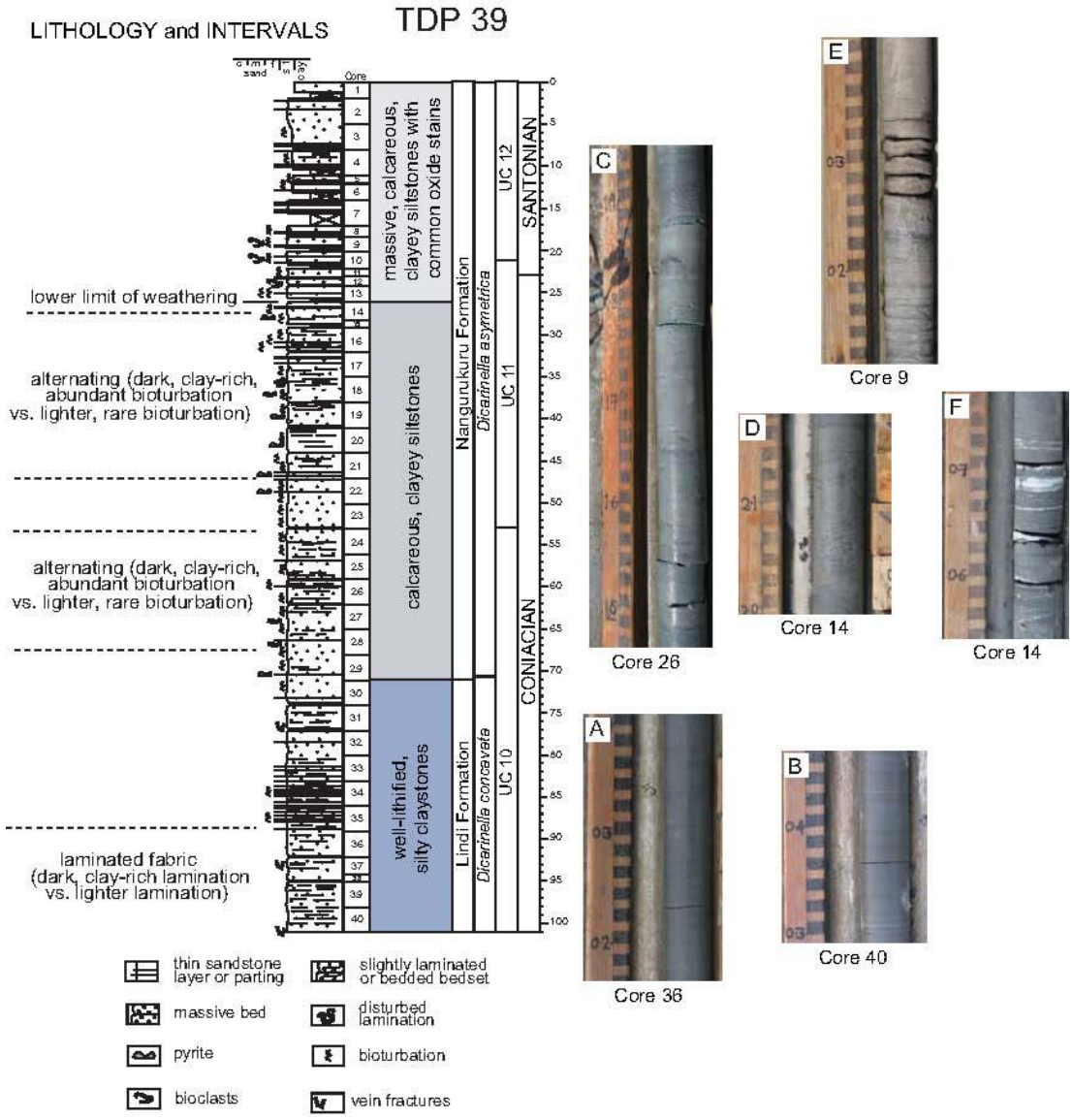

Fig 4

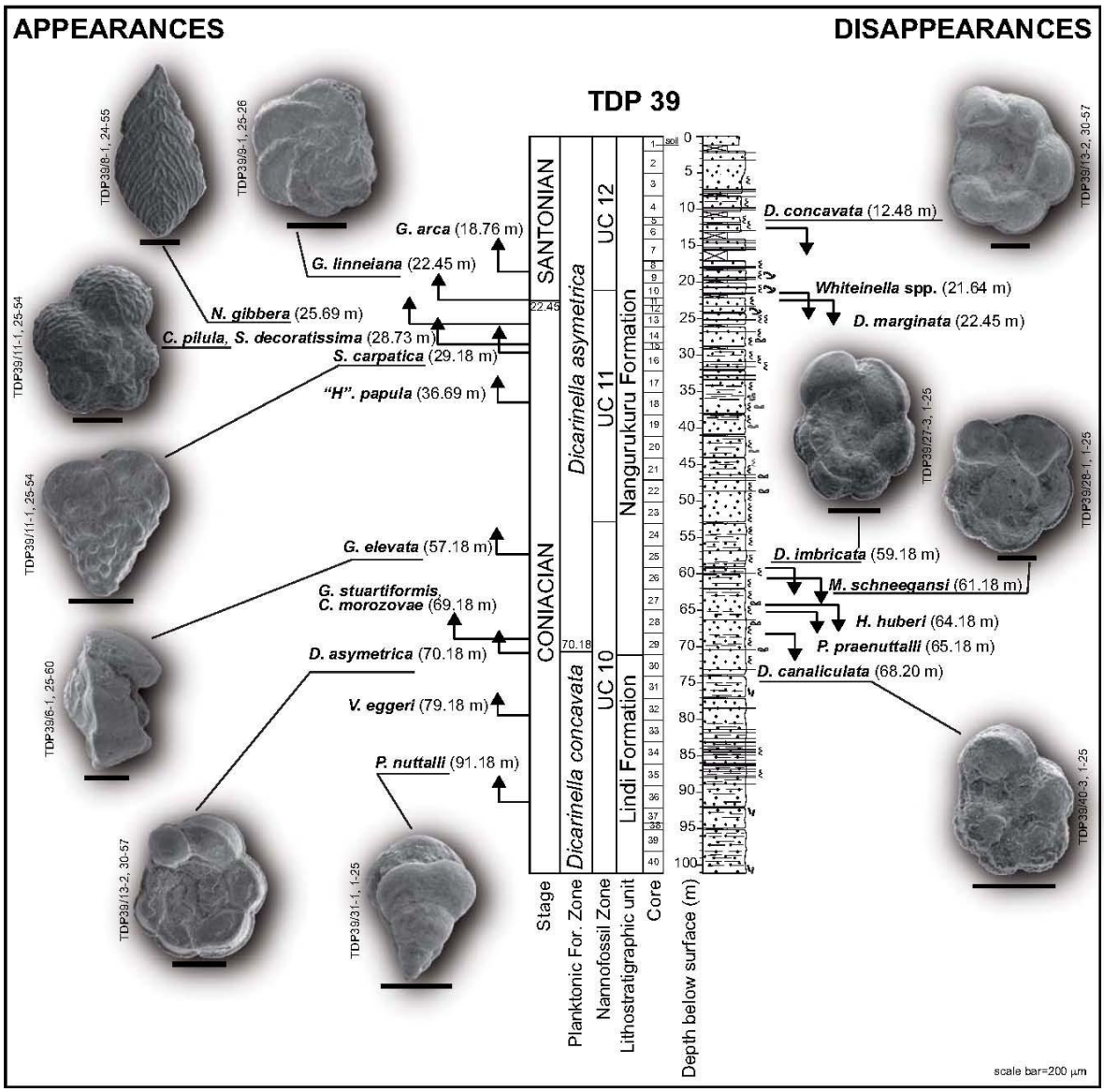

Fig. 5

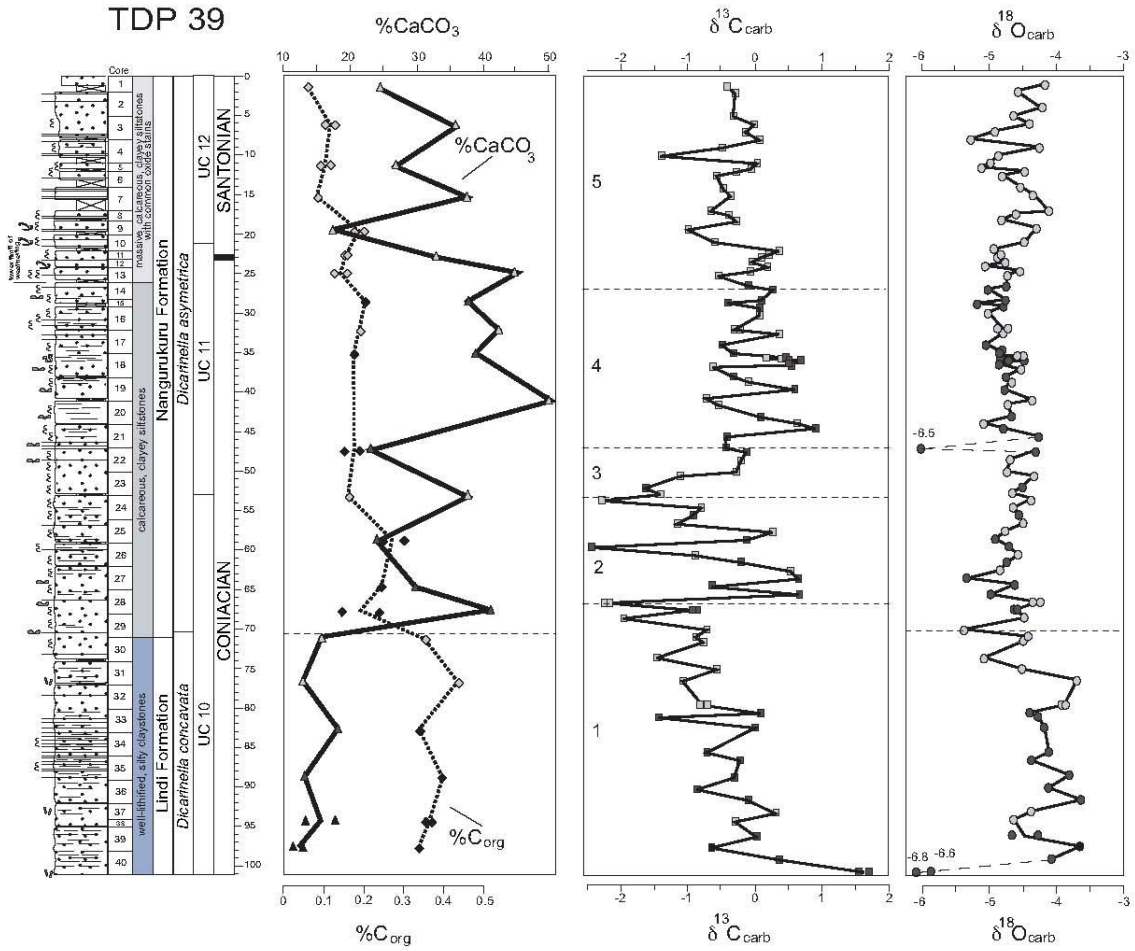

Fig. 6

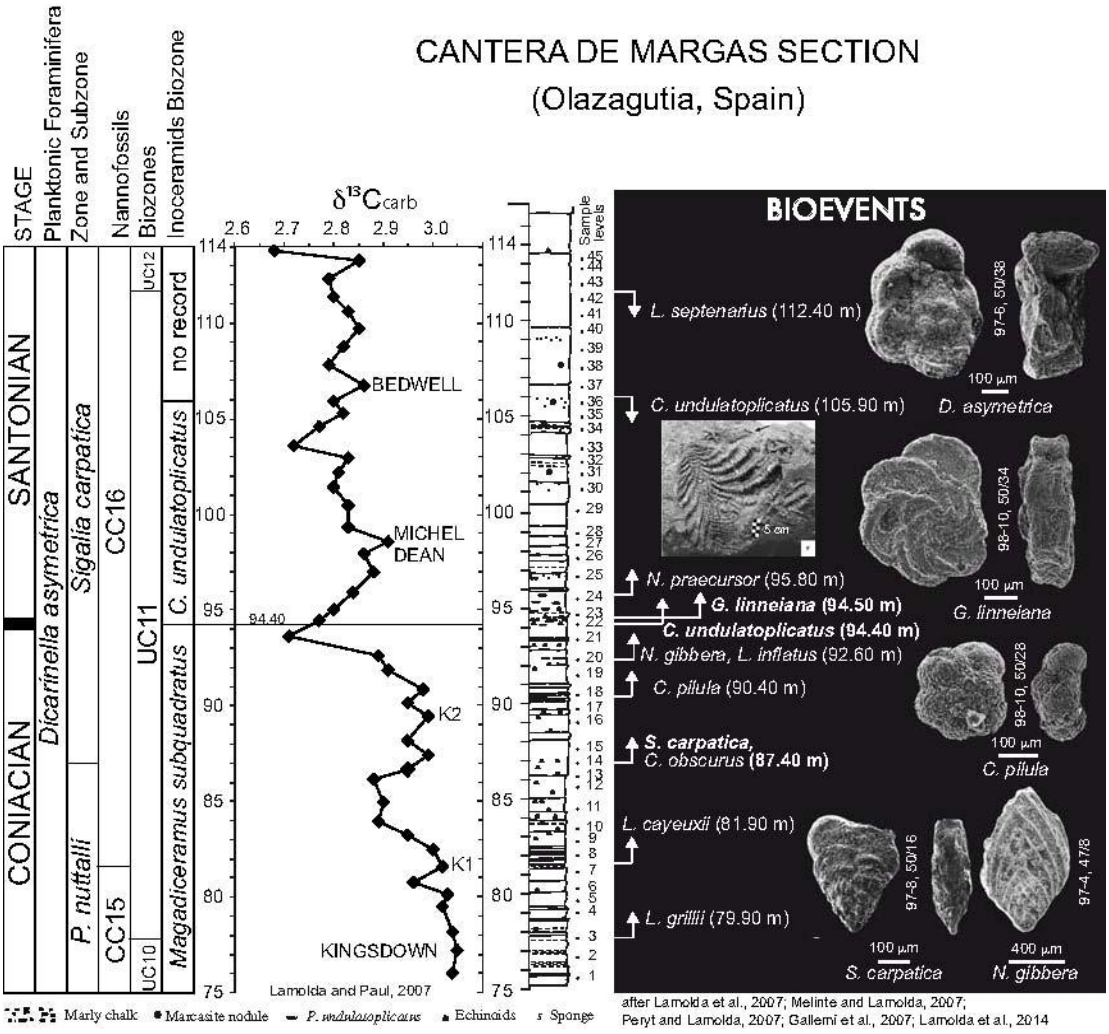

Fig. 7

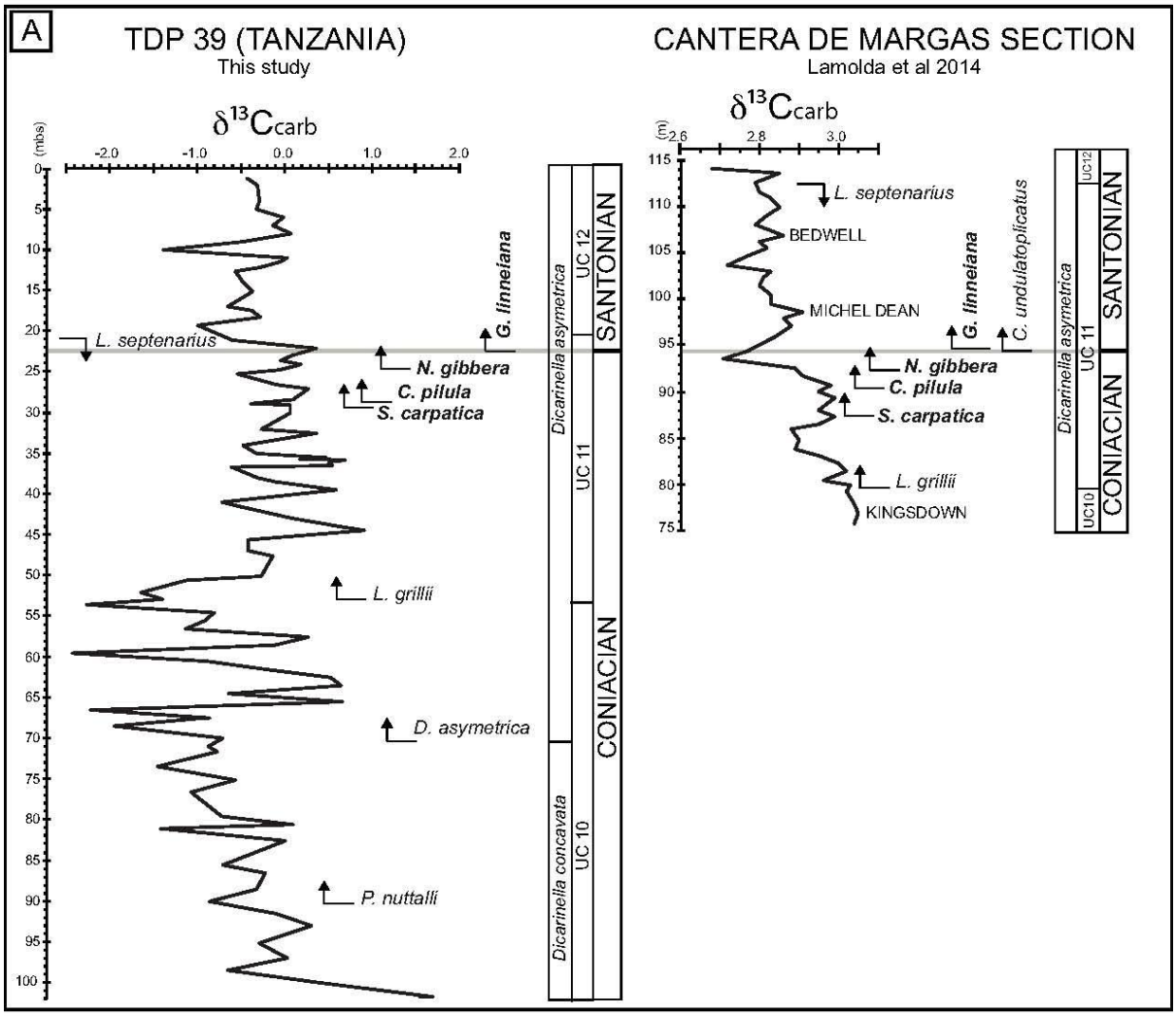

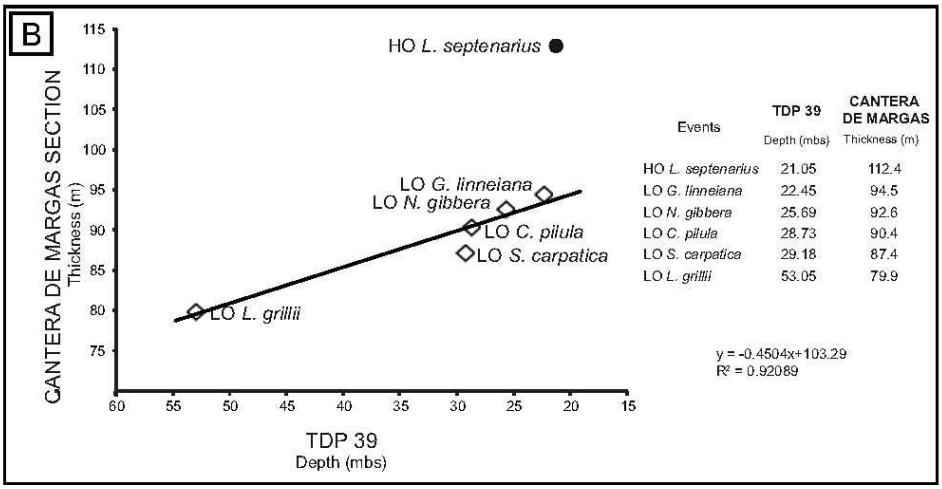

Fig. 8

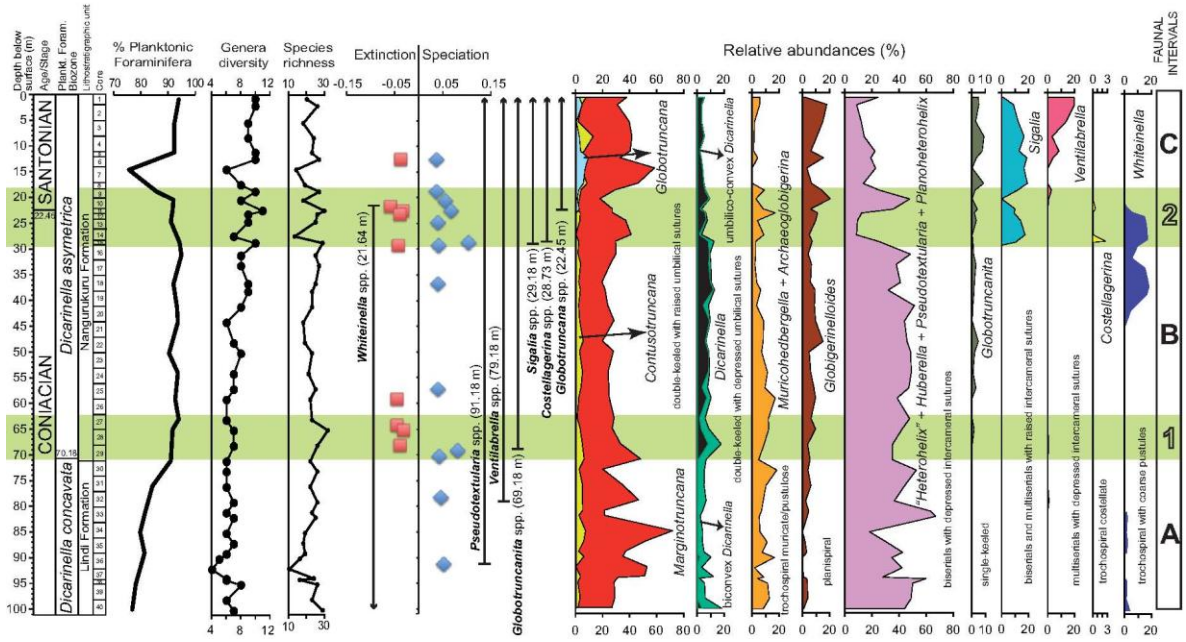

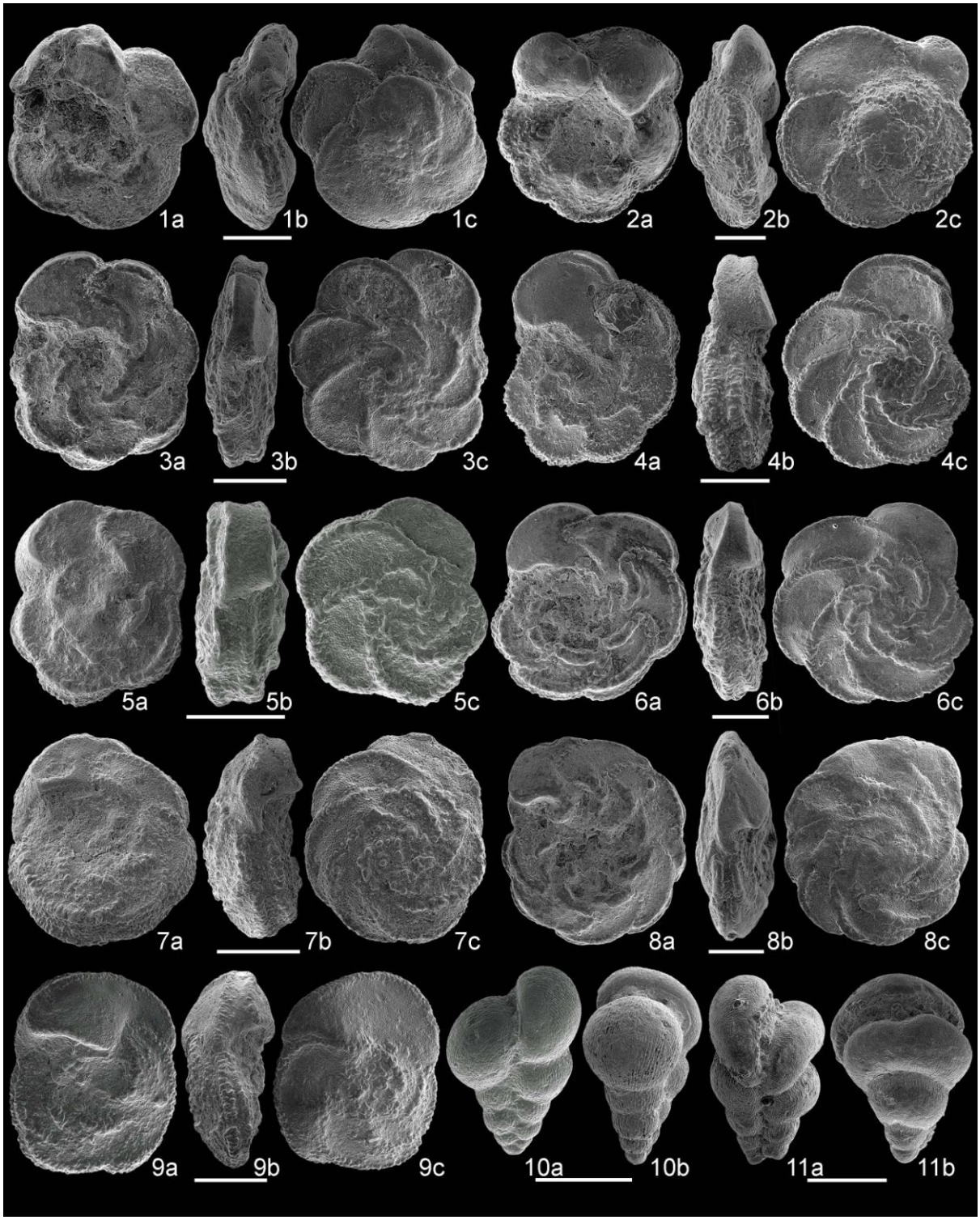

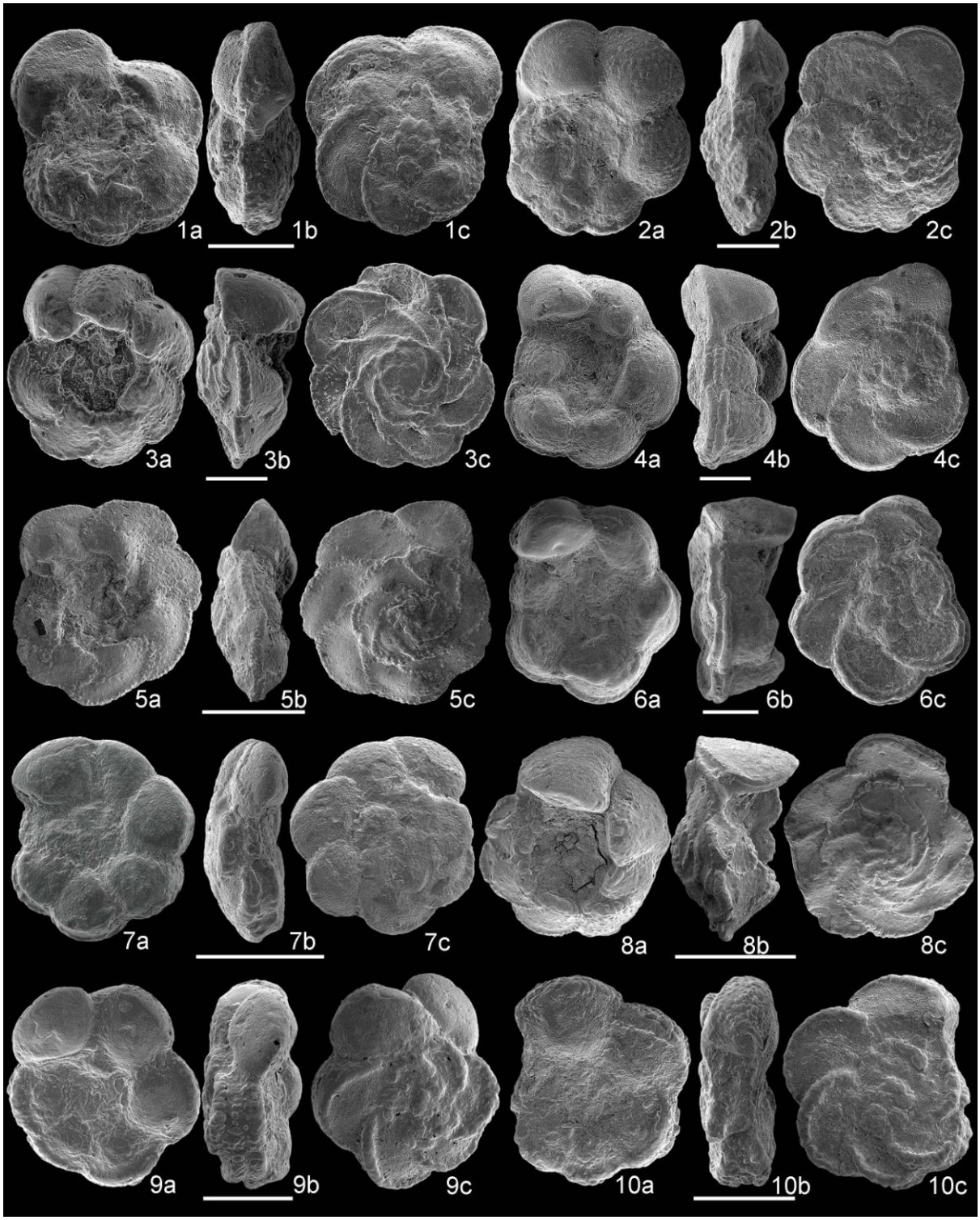

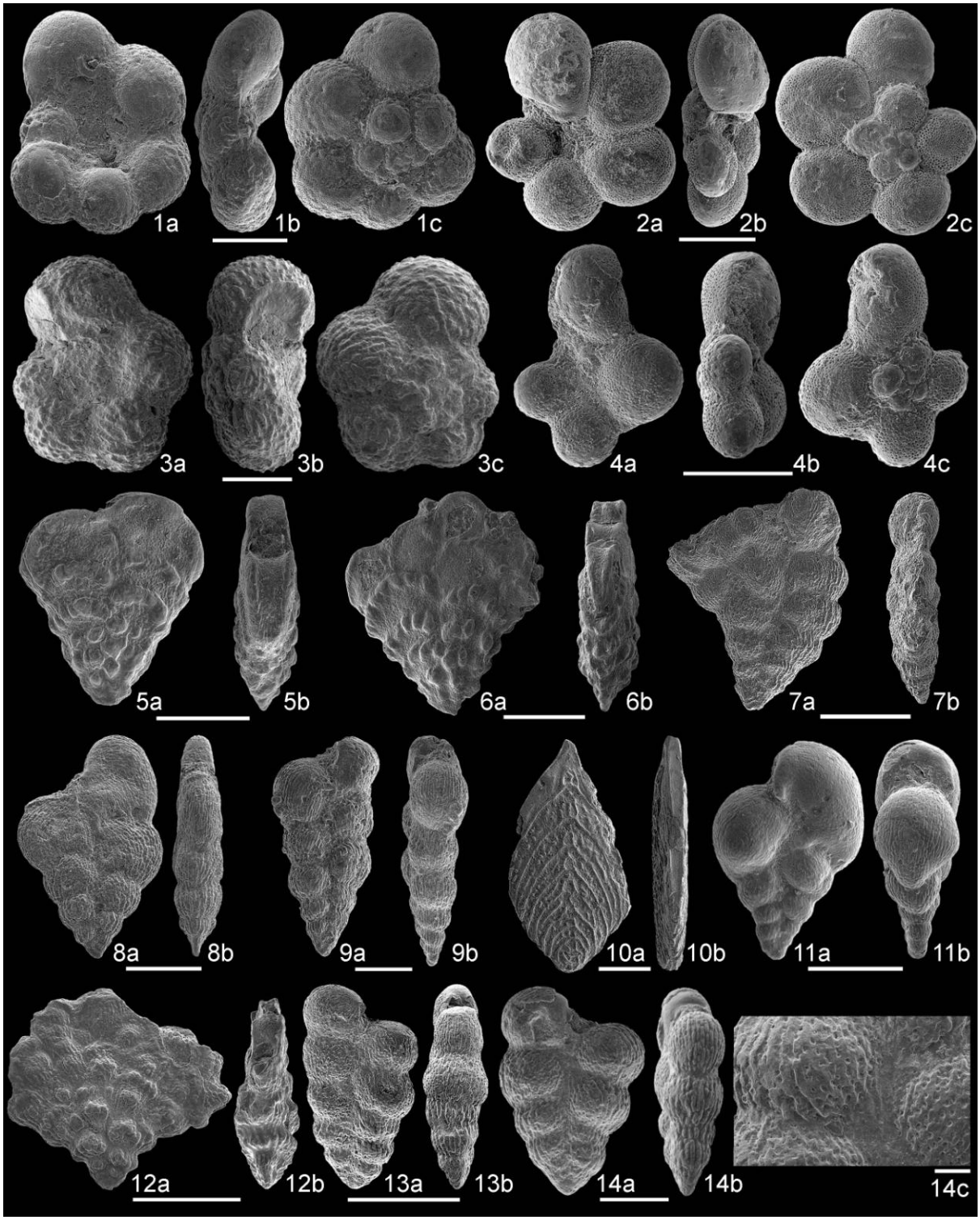

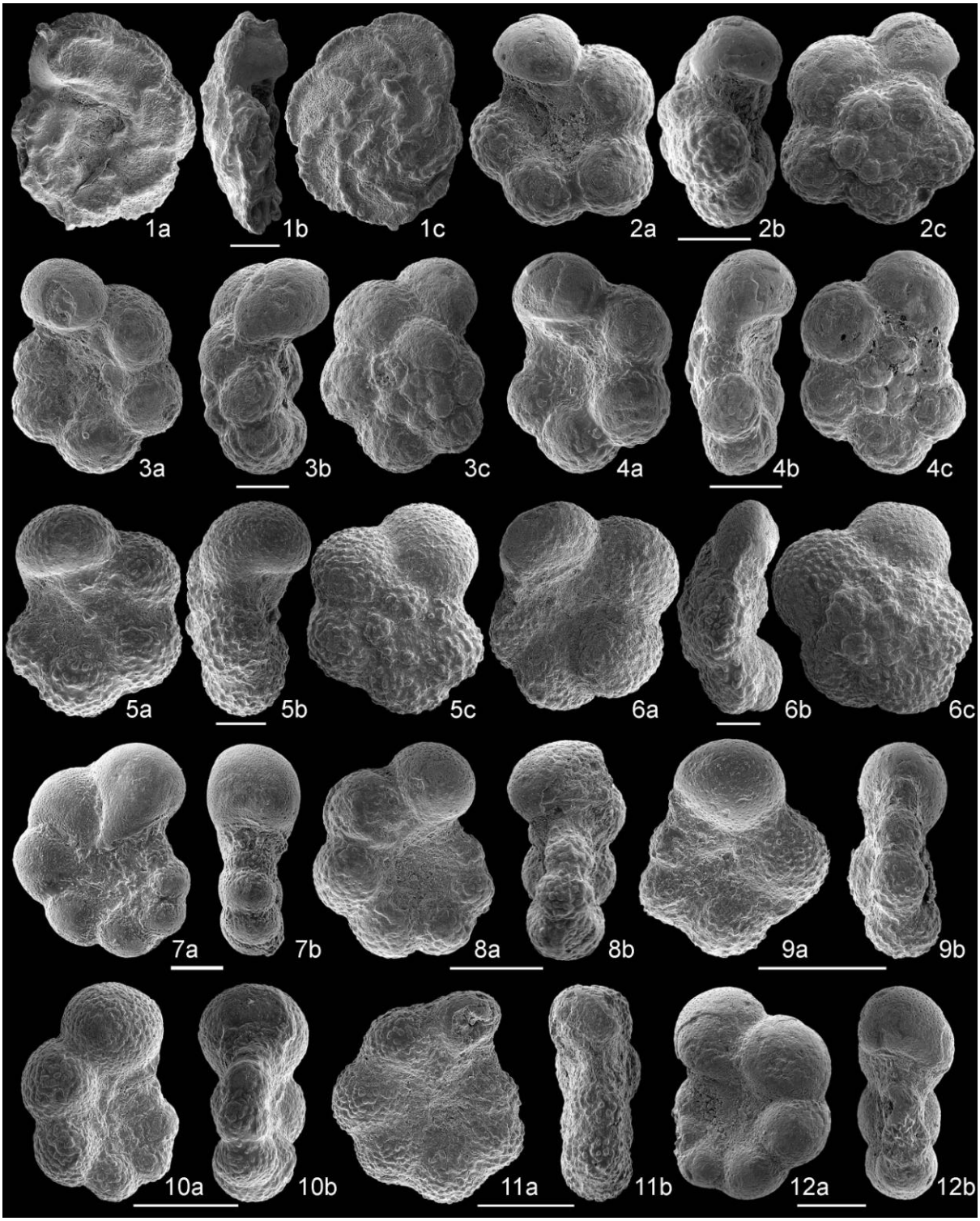

Fig. 13

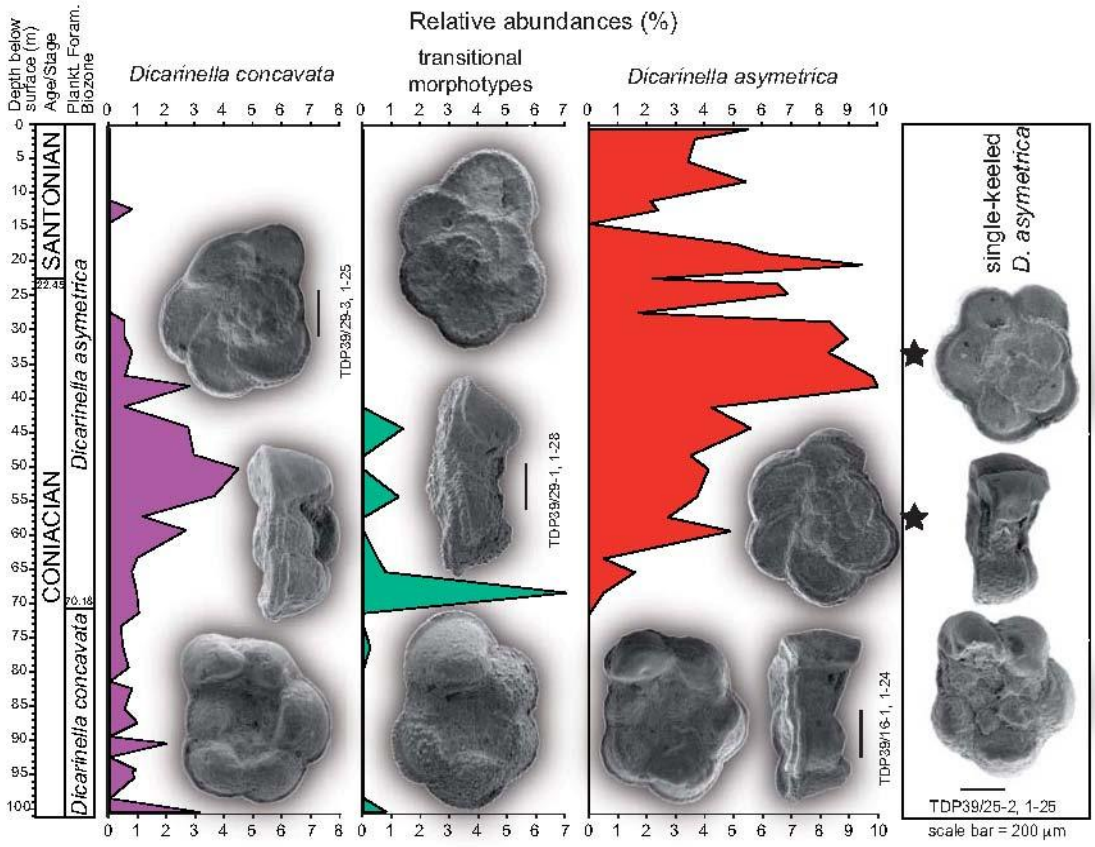

Fig. 14

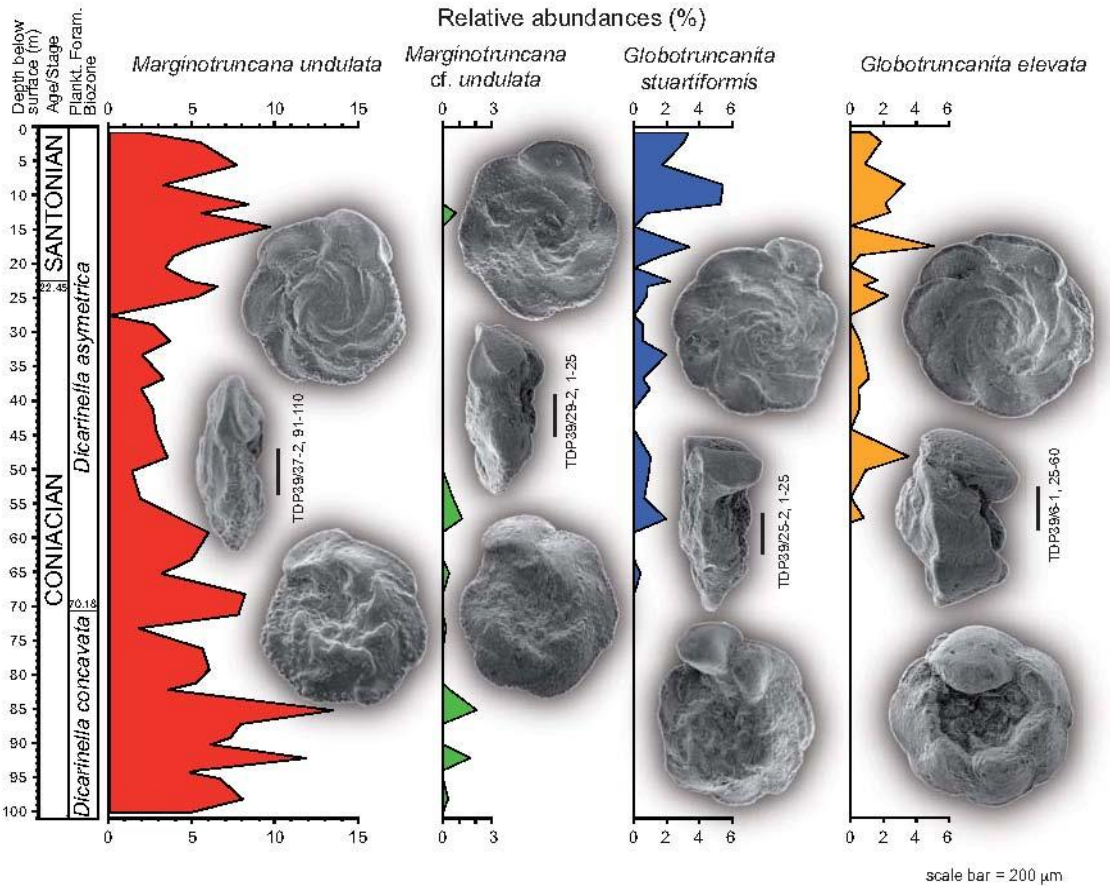

Fig. 15